Positive cross-correlations due to Dynamical Channel-Blockade in a three-terminal quantum dot

A. Cottet, W. Belzig, and C. Bruder
Department of Physics and Astronomy, University of Basel, Klingelbergstrasse 82, 4056 Basel, Switzerland
(Dated: September 19, 2006)

We investigate current fluctuations in a three-terminal quantum dot in the sequential tunneling regime. In the voltage-bias configuration chosen here, the circuit is operated like a beam splitter, i.e. one lead is used as an input and the other two as outputs. In the limit where a double occupancy of the dot is not possible, a super-Poissonian Fano factor of the current in the input lead and positive cross-correlations between the current fluctuations in the two output leads can be obtained, due to dynamical channel-blockade. When a single orbital of the dot transports current, these effects can be obtained by lifting the spin-degeneracy of the circuit with ferromagnetic leads or with a magnetic field. When several orbitals participate in the electronic conduction, lifting spin-degeneracy is not necessary. In all cases, we show that a super-Poissonian Fano factor for the input current is not equivalent to positive cross-correlations between the outputs. We identify the conditions for obtaining these two effects and discuss possible experimental realizations.

PACS numbers: 73.23.-b,72.70.+m,72.25.Rb

I. INTRODUCTION

The study of current noise in mesoscopic circuits has become a central subfield of mesoscopic physics because it allows to access informations not available through measurements of the average currents (for reviews, see Refs. [1, 2]). Current fluctuations can first be probed through the auto-correlations of the current fluctuations in one branch of the circuit. For non-interacting conductors with open channels, the fermionic statistics of electrons result in a suppression of these auto-correlations below the Poisson limit [3–5]. In a multi-terminal circuit, current fluctuations can also be probed through the cross-correlations between two different branches. Büttiker has shown that *in a non-interacting electronic circuit, the zero-frequency current cross-correlations are always negative provided the leads of the circuit are thermal reservoirs maintained at constant voltage-potentials* [6]. On the experimental side, negative cross-correlations have been measured very recently by Henny *et al.* [7] and Oliver *et al.* [8] in mesoscopic beam splitters. Oberholzer *et al.* have shown how the cross-correlations vanish in the classical limit [9].

Up to now, positive cross-correlations have never been measured in electronic circuits. However, nothing forbids to reverse the sign of cross-correlations if a hypothesis of Büttiker's proof is not fulfilled (see Ref. [10] for a recent review). First, it has been shown theoretically that positive cross-correlations can be obtained in an electronic circuit by relaxing the hypotheses of Büttiker regarding the leads, for instance by taking one of the leads superconducting [11–22], or by using leads with an imperfect [23] or time-dependent [24] voltage bias. Positive cross-correlations are also expected at finite frequencies, due to the plasmonic screening currents existing in capacitive circuits [10, 25]. It follows from Büttiker's work that obtaining positive cross-correlations at zero frequency without modifying the assumptions on the leads requires to have interactions *inside* the device. Safi *et al.* have considered a two dimensional electron gas in the fractional quantum Hall regime, described by a chiral Luttinger liquid theory [26]. Zero-frequency positive cross-correlations can be obtained in this system in the limit of small filling factors, where the excitations of the chiral Luttinger liquid take a bosonic character. This leaves open the question whether interactions localized inside the beam splitter can lead to zero-frequency positive cross-correlations even for a *normal fermionic circuit*.

Current correlations in a single quantum dot have been studied in the sequential tunneling limit [27–30], in the cotunneling regime [31, 32] and in the Kondo regime [33]. In the (spin-degenerate) sequential tunneling limit, a sub-Poissonian Fano factor has been found for some two-terminal cases [27–29], and, for the three-terminal case, cross-correlations are expected to be always negative when the intrinsic level spacing ΔE of the dot is much smaller than temperature [28]. However, a super-Poissonian Fano factor has been predicted for a two-terminal quantum dot with $\Delta E \gg k_B T$ connected to ferromagnetic leads [30]. In the cotunneling regime, a super-Poissonian Fano factor can be obtained in the two-terminal case [31]. The extent to which this would lead to positive cross-correlations for a three-terminal quantum dot was not clear.

This led us to consider, in Refs. [34, 35], the case of a three-terminal quantum dot with $\Delta E \gg k_B T$, operated as a beam splitter: one contact acts as source and the other two as drains. We have assumed that only one orbital of the dot, i.e. one single-particle level, transports current, and that Coulomb interactions prevent a double occupancy of this orbital. We have considered both the Fano factor F_2 in the input lead, called input Fano factor,

and the cross-correlations $S_{13}(\omega)$ between the two output leads, called output cross-correlations. We have proposed two different methods to obtain a super-Poissonian F_2 or $S_{13}(\omega=0)>0$ in this system, in the sequential tunneling limit. Both methods rely on lifting spin-degeneracy, either by using ferromagnetic leads [34], or by using paramagnetic leads and applying a magnetic field to the dot [35]. Note that in these works, the leads are biased with constant voltages and modeled as non-interacting Fermi gases. Then, with respect to Büttiker's proof, only the hypothesis of the absence of interactions inside the device itself is relaxed. Moreover, in contrast to the system studied in Ref. [26], excitations inside the device remain purely fermionic. Our works [34, 35] give a positive answer to the question whether zero-frequency positive cross-correlations can occur in a perfectly voltage-biased normal fermionic circuit. They nevertheless leave open the question whether lifting spin-degeneracy is necessary to do so. Eventually, it appears in [34, 35] that for certain cases, a super-Poissonian F_2 can be obtained without a positive $S_{13}(\omega=0)$. This calls for a thorough analysis of the relation between F_2 and $S_{13}(\omega=0)$.

To this end, in this article, we investigate in detail the physical origin of the positive cross-correlations found in Refs. [34, 35]. The essential ingredient is the existence of Coulomb interactions on the dot. (Note that in a spin valve connected to ferromagnetic leads, in which there are no charging effects, the cross-correlations where found to be negative [36]). In the limit where only one (singly occupied) orbital level of the dot transports current, positive cross-correlations are caused by a mechanism of *dynamical spin-blockade* which can occur when spin-degeneracy is lifted. Simply speaking, up- and down-spins tunnel through the dot with different rates. Due to the Coulomb interaction, the spins which tunnel with a lower rate modulate the transport through the opposite spin-channel, leading to a bunching of tunneling events. We show how this bunching can lead to a super-Poissonian F_2 or a positive $S_{13}(\omega=0)$. (Table (I) gives a summary of the conditions for which these properties can be obtained). In the limit of equal polarization of the output leads *and* high bias-voltage, the electronic transport is unidirectional and the division of current between the two outputs is the same for the two spin directions. This leads in the one-orbital case to a simple relation [see (25)] between F_2 and $S_{13}(\omega=0)$: a super-Poissonian F_2 is automatically associated with a positive $S_{13}(\omega=0)$. However, in general, this relation is not fulfilled even for a one-orbital dot. In particular, in the case where the leads of the one-orbital dot are paramagnetic and where spin degeneracy is lifted by a magnetic field, a positive $S_{13}(\omega=0)$ can only be obtained in an intermediary voltage range where relation (25) is not valid. This paper supplements the study of the one orbital case with an analysis of the effect of the position of the dot orbital level with respect to the zero-bias Fermi level. In the paramagnetic case, this parameters turns out to be critical to get a positive $S_{13}(\omega=0)$. An analysis of the frequency dependence of $S_{13}(\omega)$ is provided. We also show that $S_{13}(\omega=0)$ can persist in the one orbital case when the leads are magnetically polarized *and* a magnetic field applied. Eventually, we show that there is a direct mapping between this last case and that of a spin-degenerate quantum dot with two orbital levels transporting current. This mapping suggests a new way to get positive cross-correlations. In this spin-degenerate two-orbital case, positive cross-correlations stem from the partial blockade of an electronic channel by another one, thus we propose to call this effect: *dynamical channel-blockade*. This result demonstrates that *lifting spin-degeneracy is not necessary* for obtaining zero-frequency positive cross-correlations due to interactions inside a beam splitter device, even for a normal fermionic circuit with a perfect voltage bias.

Case treated in section	II	III	IV	IV	IV	V
Number of dot orbitals	1	1	1	1	1	2
Lead polarizations P_i	0	$\neq 0$	0	0	$\neq 0$	0
Magnetic field B	0	0	$\neq 0$	$\neq 0$	$\neq 0$	0
Orbital level position E_0			>0	<0		
Possibility of $S_{13}(\omega=0)>0$ or super-Poissonian F_2						
Below the high-voltage limit :		×		×	×	×
In the high-voltage limit :		×			×	×

TABLE I: Summary of the different cases of quantum dot circuits treated in this article. All these circuits have the geometry shown in Fig. 1. They differ in the number of dot orbitals implied in the current transport, the magnetic field B applied to the dot, and the magnetic polarizations P_i of the leads. In the cases marked by a cross, a super-Poissonian F_2 or a positive $S_{13}(\omega=0)$ can be obtained for appropriate values of the bias voltage V, the polarizations P_i and the tunnel rates γ_i. In the one-orbital paramagnetic case, the position E_0 of the dot orbital level with respect to the zero-bias Fermi level is also critical. Note that a super-Poissonian F_2 is not automatically associated with $S_{13}(\omega=0)>0$.

The present article is organized as follows. Section II develops the mathematical description valid for the one-orbital problem. This one-orbital problem is analyzed for two different configurations. First, the case of ferromagnetic leads and zero magnetic field is treated in Section III. Secondly, the case of a Zeeman splitting created by a magnetic field is treated in Section IV. In Section V, we show how to map the two-orbital spin-degenerate problem onto the one-orbital problem.

II. MODEL AND GENERAL DESCRIPTION FOR THE ONE-ORBITAL CASE

A. Model

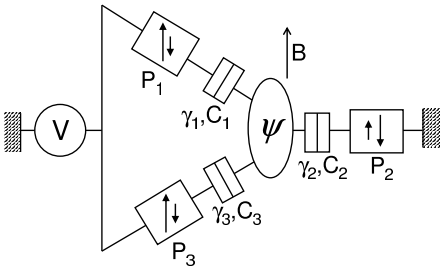

FIG. 1: Electrical diagram of a quantum dot connected to three leads $i \in \{1,2,3\}$ with collinear magnetic polarizations P_i, through tunnel junctions with net tunneling rates γ_i and capacitances C_i. A bias voltage V is applied to leads 1 and 3; lead 2 is connected to ground. A magnetic field B collinear to the lead polarizations is applied to the dot.

We consider a quantum dot connected to three leads $i \in \{1,2,3\}$, through tunnel junctions with capacitances C_i and net spin-independent tunneling rates γ_i (Fig. 1). The leads are magnetically polarized in collinear directions. We also assume that the dot is subject to a magnetic field B collinear to the lead polarizations. A voltage bias V is applied to leads 1 and 3 whereas lead 2 is connected to ground. The voltage V is considered as positive, such that it is energetically more favorable for electrons to go from the input electrode 2 to the output electrodes 1 or 3 than in the opposite direction. In this section, we also assume that

$$k_B T, \mu_B B, eV \ll E_C, \Delta E\,, \tag{1}$$

where the charging energy $E_C = e^2/2C$ of the dot depends on $C = \sum_i C_i$. According to (1), only one orbital level of the dot, with energy E_0, needs to be taken into account to describe the current transport, and this level cannot be doubly occupied. In this situation, there are three possible states ψ for the dot: either empty i.e. $\psi = 0$, or occupied with one electron with spin $\sigma \in \{\uparrow,\downarrow\}$ i.e. $\psi = \sigma$. The magnetic field B induces a Zeeman splitting of the level according to $E_{\downarrow(\uparrow)} = E_0 + (-)g\mu_B B/2$, where $\mu_B = e\hbar/2m$ is the Bohr magneton. In this article, we will assume $B \geq 0$, i.e. the up-spin level is energetically lower than the down-spin level in the presence of a magnetic field. The collinear magnetic polarizations P_j of the leads are taken into account by using *spin-dependent* tunneling rates $\gamma_{j\uparrow} = \gamma_j(1+P_j)$ and $\gamma_{j\downarrow} = \gamma_j(1-P_j)$. In a simple model, the spin-dependence is a consequence of the different densities of states for electrons with up and down spins in the leads [37]. The rate for an electron to tunnel on/off the dot ($\epsilon = +/-1$) through junction j is then given by

$$\Gamma^{\epsilon}_{j\sigma} = \gamma_{j\sigma}/(1+\exp[\epsilon(E_\sigma - eV_j)/k_B T])\,, \tag{2}$$

where $V_1 = V_3 = -C_2 V/C$ and $V_2 = (C_1+C_3)V/C$. Here, we took the Fermi energy $E_F = 0$ for lead 2 as a reference. On the dot, there can be spin-flip scattering, due for instance to spin-orbit coupling or to magnetic impurities. According to the detailed balance rule, we write the spin-flip rates as

$$\Gamma_{\uparrow\downarrow} = \gamma_{sf}\exp(+\frac{g\mu_B B}{2k_B T})$$

for the $\downarrow \longrightarrow \uparrow$ transition and

$$\Gamma_{\downarrow\uparrow} = \gamma_{sf}\exp(-\frac{g\mu_B B}{2k_B T})$$

for the $\uparrow \longrightarrow \downarrow$ transition.

B. Master equation treatment

In the sequential-tunneling limit $\hbar\gamma_{j\sigma} \ll k_B T$, electronic transport through the dot can be described by the master equation [27]

$$\frac{d}{dt}\begin{bmatrix} p_\uparrow(t) \\ p_\downarrow(t) \\ p_0(t)\end{bmatrix} = \widehat{M}\begin{bmatrix} p_\uparrow(t) \\ p_\downarrow(t) \\ p_0(t)\end{bmatrix}\,, \tag{3}$$

where $p_\psi(t)$, $\psi \in \{\uparrow,\downarrow,0\}$, is the instantaneous occupation probability of state ψ at time t, and where

$$\widehat{M} = \begin{bmatrix} -\Gamma^-_\uparrow - \Gamma_{\downarrow\uparrow} & \Gamma_{\uparrow\downarrow} & \Gamma^+_\uparrow \\ \Gamma_{\downarrow\uparrow} & -\Gamma^-_\downarrow - \Gamma_{\uparrow\downarrow} & \Gamma^+_\downarrow \\ \Gamma^-_\uparrow & \Gamma^-_\downarrow & -\Gamma^+_\uparrow - \Gamma^+_\downarrow \end{bmatrix} \tag{4}$$

depends on the total rates $\Gamma^{\epsilon}_\sigma = \sum_j \Gamma^{\epsilon}_{j\sigma}$. This master equation treatment relies on a Markovian approximation valid for frequencies ω lower than $\max[k_B T, \min_{\sigma,i}(|E_\sigma - eV_i|)]/\hbar$ [38]. From Eq. (3), the stationary occupation probabilities $\bar{p}_\psi$ are

$$\bar{p}_\sigma = \frac{\Gamma^+_\sigma\Gamma^-_{-\sigma} + \Gamma_{\sigma,-\sigma}(\Gamma^+_\uparrow + \Gamma^+_\downarrow)}{\gamma_\uparrow\gamma_\downarrow - \Gamma^+_\uparrow\Gamma^+_\downarrow + \sum_{\sigma'}(\gamma_{\sigma'} + \Gamma^+_{-\sigma'})\Gamma_{\sigma',-\sigma'}}\,, \tag{5}$$

with $\gamma_\sigma = \sum_j \gamma_{j\sigma}$, for $\sigma \in \{\uparrow,\downarrow\}$, and

$$\bar{p}_0 = 1 - \bar{p}_\uparrow - \bar{p}_\downarrow\,. \tag{6}$$

These probabilities can be used to calculate the average value $\langle I_j\rangle$ of the tunneling current $I_j(t)$ through junction j as $\langle I_j\rangle = \sum_\sigma \langle I_{j,\sigma}\rangle$, where $\langle I_{j,\sigma}\rangle = \sum_\epsilon \langle I^{\epsilon}_{j,\sigma}\rangle$ is the average current of electrons with spins σ, and

$$\langle I^{\epsilon}_{j,\sigma}\rangle = e\epsilon\Gamma^{\epsilon}_{j\sigma}\bar{p}_{A(\sigma,-\epsilon)}\,. \tag{7}$$

Here, $A(\sigma,\epsilon)$ is the state of the dot after the tunneling of an electron with spin σ in the direction ϵ, i.e. $A(\sigma,-1)=0$ and $A(\sigma,+1)=\sigma$.

The frequency spectrum of the noise correlations can be defined as

$$S_{ij}(\omega)=\int_{-\infty}^{+\infty}dt\mathcal{C}_{ij}(t)\exp(i\omega t)\,, \tag{8}$$

where

$$\mathcal{C}_{ij}(t)=\langle\Delta I_i(t)\Delta I_j(0)\rangle+\langle\Delta I_i(0)\Delta I_j(t)\rangle \tag{9}$$

and $\Delta I_i(t)=I_i(t)-\langle I_i\rangle$. Following the method developed in Refs. [27], we can write this spectrum as:

$$S_{ij}(\omega)=\delta_{ij}S_j^{Sch}+S_{ij}^c(\omega) \tag{10}$$

with $S_j^{Sch}=\sum_\sigma S_{j\sigma}^{Sch}$ and $S_{ij}^c(\omega)=\sum_{\sigma,\sigma'}S_{i\sigma,j\sigma'}^c(\omega)$. Here,

$$S_{j\sigma}^{Sch}=2e\sum_\epsilon\left|\langle I_{j,\sigma}^\epsilon\rangle\right| \tag{11}$$

is the Schottky noise associated to the tunneling of electrons with spin σ through junction j, and, from (3),

$$\frac{S_{i\sigma,j\sigma'}^c(\omega)}{2e^2}=\sum_{\epsilon,\epsilon'}\epsilon\epsilon'\left[\Gamma_{i\sigma}^{\epsilon'}\widehat{\mathcal{G}}_{A(\sigma,-\epsilon'),A(\sigma',\epsilon)}(\omega)\Gamma_{j\sigma'}^{\epsilon}\bar{p}_{A(\sigma',-\epsilon)}\right. \tag{12}$$

$$\left.+\Gamma_{j\sigma'}^{\epsilon'}\widehat{\mathcal{G}}_{A(\sigma',-\epsilon'),A(\sigma,\epsilon)}(-\omega)\Gamma_{i\sigma}^{\epsilon}\bar{p}_{A(\sigma,-\epsilon)}\right]\,,$$

with

$$\widehat{\mathcal{G}}(\omega)=-\,\mathrm{Re}\left[\left(i\omega\widehat{I}+\widehat{M}\right)^{-1}\right] \tag{13}$$

and $\widehat{I}$ the identity matrix. We also define, for later use, the spin components of $S_{ij}(\omega)$:

$$S_{i\sigma,j\sigma'}(\omega)=\delta_{ij}\delta_{\sigma\sigma'}S_{i\sigma}^{Sch}+S_{i\sigma,j\sigma'}^c(\omega)\,. \tag{14}$$

Due to the existence of the stationary solution $\widehat{M}\bar{p}_0=0$, the matrix $\widehat{M}$ has only two non-zero eigenvalues λ_+ and λ_-, i.e. $\widehat{M}v_\pm=\lambda_\pm v_\pm$, given by

$$\lambda_\pm=\frac{1}{2}\left(-\Lambda\pm\sqrt{\Lambda^2-4\Theta}\right)<0\,,$$

with

$$\Lambda=\Gamma_{\uparrow\downarrow}+\Gamma_{\downarrow\uparrow}+\gamma_\uparrow+\gamma_\downarrow$$

and

$$\Theta=\gamma_\uparrow\gamma_\downarrow+\Gamma_{\uparrow\downarrow}\left(\Gamma_\downarrow^+\gamma_\uparrow\right)+\Gamma_{\downarrow\uparrow}\left(\gamma_\downarrow+\Gamma_\uparrow^+\right)-\Gamma_\uparrow^+\Gamma_\downarrow^+\,.$$

Then, the matrix $\widehat{M}$ can be written in the form $\widehat{M}=\widehat{R}^{-1}\left(\lambda_+\widehat{E}_+-\lambda_-\widehat{E}_-\right)\widehat{R}$, where $\widehat{R}$ is a reversible 3×3 matrix, and $\widehat{E}_{+(-)}$ is a 3×3 matrix with the element 1 at the first (second) row and first (second) column. Accordingly, $\widehat{\mathcal{G}}(\omega)$ can be written as

$$\widehat{\mathcal{G}}(\omega)=\frac{\widehat{\mathcal{A}}^+}{\omega^2+\lambda_+^2}+\frac{\widehat{\mathcal{A}}^-}{\omega^2+\lambda_-^2}\,, \tag{15}$$

with $\widehat{\mathcal{A}}^\pm=-\lambda_\pm\widehat{R}^{-1}\widehat{E}_\pm\widehat{R}$. Therefore, we have

$$S_{ij}^c(\omega)=\sum_{s=\pm}\frac{S_{ij}^s}{\omega^2+\lambda_s^2}\,, \tag{16}$$

where S_{ij}^s follows from Eqs. (12) and (15). The total Schottky noise S_j^{Sch} through junction j is a white noise due to the hypothesis of instantaneous tunneling. For a single junction biased by a voltage source, one would get only this term. However, in the spectrum $S_{ij}(\omega)$, interactions don't come into play only through the frequency dependent term (16). Interactions also modify the values of the terms $\langle I_{j\sigma}^\epsilon\rangle$ determining the Schottky noise. Note that at high frequencies $\omega\gg|\lambda_-|$, we have $S_{ij}(\omega)=\delta_{ij}S_j^{Sch}$. If we furthermore assume $V\gg V_{\max}^{sgn(E_0)}$, $S_j^{Sch}=2e\left|\langle I_j\rangle\right|$ thus $S_{ij}(\omega)$ becomes Poissonian, i.e. $S_{ij}(\omega)=2e\left|\langle I_i\rangle\right|\delta_{ij}$.

In the three-terminal case studied here, we will be interested in the input Fano factor

$$F_2=\frac{S_{22}(\omega=0)}{2e\langle I_2\rangle}\,,$$

and in the output cross-Fano factor

$$F_{13}=\frac{S_{13}(\omega=0)}{2e\langle I_2\rangle}\,.$$

We also define the resonance voltages

$$V_0^-=|E_0|\frac{C}{eC_2}$$

and

$$V_0^+=|E_0|\frac{C}{e(C_1+C_3)}\,.$$

Since we consider $V>0$ only, at $B=0$, for E_0 positive (negative), the dot orbital arrives at resonance with the Fermi level of the input (the outputs) when $V\simeq V_0^{+(-)}$. If a magnetic field is applied, each of these voltage resonances is split into two resonances

$$V_{\uparrow(\downarrow)}^-=V_0^-+(-)\frac{g\mu_BBC}{2eC_2}$$

and

$$V_{\uparrow(\downarrow)}^+=V_0^+-(+)\frac{g\mu_BBC}{2e(C_1+C_3)}\,,$$

associated to the $\uparrow$ ($\downarrow$) levels respectively because we consider $B > 0$ only. We expect F_2 and F_{13} to show strong variations for $V \simeq V_{\uparrow(\downarrow)}^{sgn(E_0)}$.

C. Time-domain analysis

The correlation function $\mathcal{C}_{ij}(t)$ can be obtained from the inverse Fourier transform of Eqs. (10), (11) and (16):

$$\mathcal{C}_{ij}(t) = \delta_{ij}\delta(t)S_j^{Sch} + \sum_{s=\pm} \frac{S_{ij}^s}{2\left|\lambda_s\right|} \exp(-\left|t\right|\left|\lambda_s\right|) \ . \quad (17)$$

In the sequential tunneling limit, tunneling events occur one by one, thus

$$\lim_{t\to 0^+} \mathcal{C}_{ij}(t) = -2\left\langle I_i\right\rangle\left\langle I_j\right\rangle < 0 \ . \quad (18)$$

Let us first focus on the spin-degenerate case, that is $\Gamma_{j\uparrow}^{\epsilon} = \Gamma_{j\downarrow}^{\epsilon}$ for $j \in \{1,2,3\}$. In this case, the eigenvectors $v_{+/-}$ of $\widehat{M}$ correspond to the spin/charge excitations of the system (i.e. $v_+ \sim [1,-1,0]$, $v_- \sim [1,1,-2]$), and $\lambda_{+/-}$ to their relaxation rates. This is directly connected to the fact that in the spin-degenerate case, $S_{ij}^+ = 0$, thus $S_{ij}(\omega) - \delta_{ij}S_j^{Sch}$ is a Lorentzian function and $\mathcal{C}_{ij}(t) - \delta_{ij}\delta(t)S_j^{Sch} = S_{ij}^- \exp(-\left|t\right|\left|\lambda_-\right|)/2\left|\lambda_-\right|$. This last equation implies that, for any time, $\mathcal{C}_{22}(t) - \delta(t)S_2^{Sch}$ and $\mathcal{C}_{13}(t)$ keep the same sign, which is negative according to Eq. (18). Thus, *in the spin-degenerate one-orbital case, F_2 is always sub-Poissonian and F_{13} always negative.* When spin-degeneracy is lifted, $v_{+/-}$ both become a linear combination of the charge and spin excitations. Thus, having $S_{ij}^+ \neq 0$ is not forbidden anymore. Eqs. (17), and (18) altogether with $|\lambda_+| < |\lambda_-|$ imply that if $S_{ij}(\omega = 0) > \delta_{ij}S_j^{Sch}$, one has $S_{ij}^- < 0$ and $S_{ij}^+ > 0$. Therefore, in the one-orbital case, a positive sign for $F_2 - S_2^{Sch}/2e\left\langle I_2\right\rangle$ and F_{13} can only be due to terms in λ_+.

The results obtained for $\mathcal{C}_{ij}(t)$ can be put in perspective with some fundamental quantities like the average dwell time t_σ of spins σ on the dot and the average delay t_0 between the occupancy of the dot by two consecutive electrons. These quantities can be calculated for $\gamma_{sf} = 0$ as

$$t_\sigma = \frac{4e^2\bar{p}_\sigma}{\sum_j S_{j,\sigma}^{Sch}} \quad (19)$$

and

$$t_0 = \frac{4e^2\bar{p}_0}{\sum_j S_j^{Sch}} \ . \quad (20)$$

The noise reaches its high-voltage limit once $V \gg V_{\max}^{sgn(E_0)} = \max_\sigma(V_\sigma^{sgn(E_0)})$ with $V_{\max}^+ = V_\downarrow^+$ and $V_{\max}^- = V_\uparrow^-$. In this limit, the current transport is unidirectional, i.e. $\left\langle I_{2,\sigma}^-\right\rangle = 0$ and $\left\langle I_{j,\sigma}^+\right\rangle = 0$ and for any $j\times\sigma \in \{1,3\}\times\{\uparrow,\downarrow\}$. Thus, Eqs. (19) and (20) lead to $t_0 = 1/2\gamma_2$ and $t_\sigma = 1/\left(\gamma_{1\sigma} + \gamma_{3\sigma}\right)$. The average number

$$n_b = \frac{S_{2\uparrow}^{Sch}}{S_{2\downarrow}^{Sch}} \quad (21)$$

of up spins crossing the input junction between two consecutive down spins for $\gamma_{sf} = 0$, which becomes $n_b = I_{2\uparrow}/I_{2\downarrow}$ for $V \gg V_{\max}^{sgn(E_0)}$, is also of importance. It can be used to calculate the average duration

$$t_b = n_b t_\uparrow + (n_b + 1)\, t_0 \quad (22)$$

between the occupation of the dot by two consecutive down spins for $\gamma_{sf} = 0$. In Section III.C, the analysis of $\mathcal{C}_{ij}(t)$ will be supplemented by simulating numerically the time evolution of the spin σ_{dot} of the dot. As expected, these simulations are in agreement with the results obtained from the master equation approach, but their interest is to allow a visualization of $\sigma_{dot}(t)$.

D. Relation between F_2 and F_{13}

The average input current $\left\langle I_2\right\rangle$ and the input Fano factor F_2 in a three-terminal device correspond to the average current and the Fano factor in a two-terminal device where the output leads 1 and 3 are replaced by an effective output with a net spin-independent tunneling rate $\gamma_t = \gamma_1 + \gamma_3$ and with an effective polarization $P_{out} = \left(\gamma_1 P_1 + \gamma_3 P_3\right)/\gamma_t$. Then, one fundamental question to answer is whether there is a simple relation between F_2 and F_{13} in the three-terminal circuit. Charge conservation and the finite dispersion of $|\sigma_{dot}(t)|$ lead to [27]

$$S_{22}\left(\omega = 0\right) = S_{11}\left(\omega = 0\right) + S_{33}\left(\omega = 0\right) + 2S_{13}\left(\omega = 0\right) \ . \quad (23)$$

At high voltages $V \gg V_{\max}^{sgn(E_0)}$, the unidirectionality of current transport and the average-currents conservation lead to $S_2^{Sch} = S_1^{Sch} + S_3^{Sch}$. In this limit, Eqs. (10) and (23) imply that

$$S_{22}^c\left(\omega = 0\right) = S_{11}^c\left(\omega = 0\right) + S_{33}^c\left(\omega = 0\right) + 2S_{13}^c\left(\omega = 0\right) \ . \quad (24)$$

Since the voltage bias is the same for leads 1 and 3, we have $\Gamma_{3,\sigma}^{\epsilon}/\Gamma_{1,\sigma}^{\epsilon} = \gamma_{1\sigma}/\gamma_{3\sigma}$ for $\epsilon = \pm 1$. Then, in our singly-occupied one-orbital case, Eqs. (12) and (24) lead to

$$S_{22}^c\left(\omega = 0\right) = \sum_{\sigma,\sigma'} \frac{\left(\gamma_{1\sigma} + \gamma_{3\sigma}\right)\left(\gamma_{1\sigma'} + \gamma_{3\sigma'}\right)}{\gamma_{1\sigma}\gamma_{3\sigma'}} S_{1,\sigma,3,\sigma'}^c\left(\omega = 0\right) \ .$$

If we furthermore assume $P_1 = P_3$, the ratio $\gamma_{1\sigma}/\gamma_{3\sigma} = \gamma_1/\gamma_3$ is independent of σ and

$$F_{13} = (F_2 - 1)\,\frac{\gamma_1\gamma_3}{\gamma_t^2}\ . \qquad (25)$$

In summary, for the one-orbital circuit studied here, there exists a simple relation between F_2 and F_{13} when $P_1 = P_3$ and $V \gg V_{\max}^{sgn(E_0)}$. Note that the derivation of property (25) requires neither $\gamma_{sf} = 0$, nor $B = 0$. On the contrary, the voltage-bias configuration used is crucial. Indeed, if the three leads 1, 2, 3, were for instance biased at voltages V, $V/2$ and 0 respectively, the current transport would not be unidirectional even in the high V-limit. When property (25) is verified, a super-Poissonian (sub-Poissonian) F_2 is automatically associated with positive (negative) zero-frequency cross-correlations. However, Sections III and IV, which also treat this one-orbital case, illustrate that when $P_1 \neq P_3$ or $V \lesssim V_{\max}^{sgn(E_0)}$, property (25) is not valid anymore, and in particular a super-Poissonian F_2 can be obtained without a positive F_{13}. In Section IV.B, F_2 and F_{13} even show variations which are *qualitatively* different: F_{13} displays a voltage resonance not present in F_2. Thus, even for the one-orbital quantum dot circuit studied here, the three-terminal problem is in general not trivially connected to the two-terminal problem.

The main ingredients for deriving (25) are the unidirectionality of current transport and a division of current between the two outputs identical for the two spin directions. One can wonder whether any tunnel-junction circuit with a geometry analogous to that of Figure 1 satisfies property (25) for $V \gg V_{\max}^{sgn(E_0)}$ and $P_1 = P_3$. Indeed, it is sometimes the case. For instance, Börlin *et al.* have studied at $T = 0$ a normal-metal island too large to have charging effects, connected, through tunnel junctions, to one superconducting or normal input lead and to two normal output leads with $P_1 = P_3 = 0$ placed at the same output potential [17]. For this system, in both the hybrid and the normal cases, a relation analog to (25) is fulfilled, provided γ_1/γ_3 is replaced by g_1/g_3, where g_1 and g_3 are the conductances of the output junctions. In spite of this, (25) is not universal even for *spin-degenerate* tunnel-junction circuits. This can be shown by considering the circuit of Fig. 1, with $B = 0$, $P_1 = P_2 = P_3 = 0$ and a *two-orbital* dot (Section V). In this case, the division of currents between the two outputs will generally depend on the orbital considered, because of the different spatial extensions of the orbitals and of the asymmetric positions of the output leads with respect to them [39]. One has to assume that the division of currents between leads 1 and 3 is independent of the orbital considered in order to recover property (25) at $V \gg V_{\max}^{sgn(E_0)}$.

E. Influence of screening currents at non-zero frequencies

The total instantaneous current $I_j^{tot}(t)$ passing through branch j includes the tunneling current $I_j(t)$ but also the screening currents needed to guarantee the electrostatic equilibrium of the capacitors after a tunneling event through any junction $i \in \{1, 2, 3\}$. However, screening currents contribute neither to the average value $\langle I_j^{tot}\rangle$ of the total current $I_j^{tot}(t)$, i.e. $\langle I_j^{tot}\rangle = \langle I_j\rangle$, nor to the low frequency part of the total current correlations $S_{ij}^{tot}(\omega)$, i.e. $S_{ij}^{tot}(\omega) = S_{ij}(\omega = 0)$ for $|\omega| \ll |\lambda_+|$, because, in average, the screening currents due to tunneling through the different junctions compensate each other at zero frequency (see for instance [1]). Screening currents contribute to $S_{ij}^{tot}(\omega)$ only once $S_{ij}(\omega)$ deviates from its zero-frequency limit. In the following, we will assume that the cutoff frequency $|\lambda_+|$ is much larger than the inverse of the collective response times associated to the charging of the capacitors. This is equivalent to assuming that, on the time scale on which $\sigma_{dot}(t)$ varies, any charge variation of the dot triggers instantaneously the screening currents needed for its compensation:

$$I_j^{tot}(t) = I_j(t) - \frac{C_j}{C}\sum_i I_i(t)\ . \qquad (26)$$

According to this approximation, the total current correlations $S_{ij}^{tot}(\omega)$, including screening currents, can be written as

$$S_{ij}^{tot}(\omega) = \sum_{n,m}\left(\delta_{in} - \frac{C_i}{C}\right)\left(\delta_{jm} - \frac{C_j}{C}\right) S_{nm}(\omega)\ . \qquad (27)$$

The sign of these total current cross-correlations is not trivial. This problem is addressed in Section III.E.

III. ONE-ORBITAL QUANTUM DOT CONNECTED TO FERROMAGNETIC LEADS, IN THE ABSENCE OF A MAGNETIC FIELD

Here, we focus on the one-orbital case introduced in Section II, for $B = 0$ and magnetically polarized leads. In the absence of a magnetic field, one single resonance is expected in the voltage characteristics, for $V \simeq V_0^{sgn(E_0)}$. Figures 2 to 7 show curves for a constant value of the polarization amplitudes $|P_1| = |P_2| = |P_3| = 0.6$. This corresponds for instance to having the different leads made out of the same ferromagnetic material.

A. Zero-frequency results for $E_0 > 0$

We first consider the case in which the orbital level E_0 is above the Fermi level of the leads at equilibrium ($E_0 > 0$). The typical voltage dependence of the average

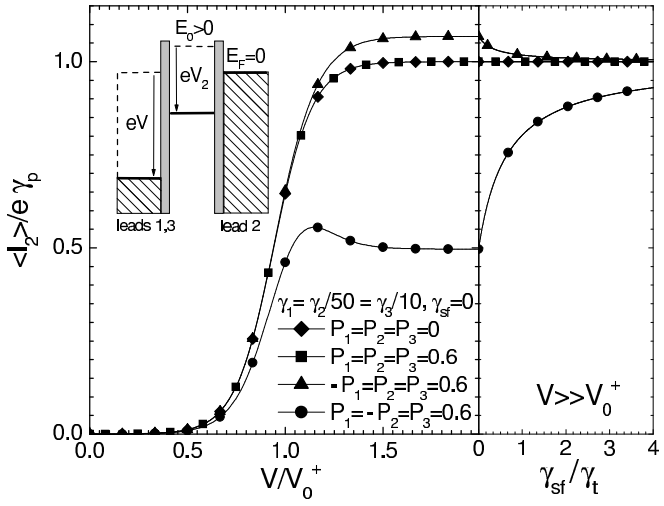

FIG. 2: Left panel: Current-voltage characteristic of the circuit of Fig. 1, for $E_0 > 0$, $C_1 = C_2 = C_3$, $\gamma_1 = \gamma_2/50 = \gamma_3/10$, $k_BT/|E_0| = 0.1$, $B = 0$, and different values of lead polarizations. The average current $\langle I_2\rangle$ through lead 2 is plotted in units of its paramagnetic high voltage limit $e\gamma_p = 2e\gamma_2\gamma_t/(\gamma_t+2\gamma_2)$ with $\gamma_t = \gamma_1+\gamma_3$; the voltage in units of the resonance voltage V_0^+ (see II.B). For $P_1 = P_2 = P_3$ (squares), $\langle I_2\rangle$ coincides with the paramagnetic case (diamonds). In the other cases, the high-voltage limit of $\langle I_2\rangle$ can be larger or smaller than the paramagnetic value, depending on the lead polarizations. The inset shows the electrochemical potentials in the circuit. Notation E_F refers to the Fermi level in lead 2. (In all the plots, potentials are shown for the case where the dot is empty**)**. Right panel: Influence of spin-flip scattering in the high-voltage limit $V \gg V_0^+$. Here, the spin flip scattering rate γ_{sf} is expressed in units of γ_t. Spin-flip scattering makes the $\langle I_2\rangle(V)$ curve tend to the paramagnetic one.

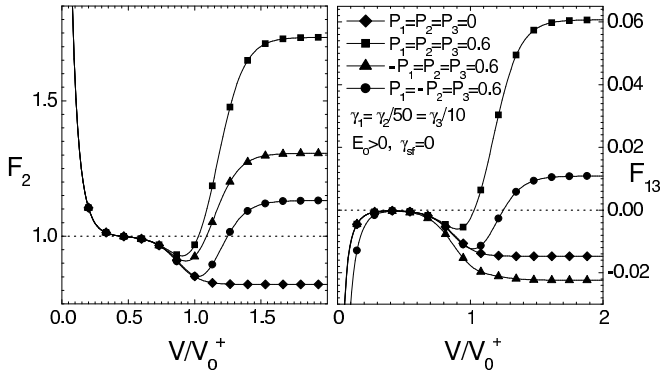

FIG. 3: Input Fano factor $F_2 = S_{22}(\omega = 0)/2eI_2$ (left panel) and output cross-Fano factor $F_{13} = S_{13}(\omega = 0)/2eI_2$ between leads 1 and 3 (right panel) as a function of the bias voltage V for $\gamma_{sf} = 0$. The curves are shown for the same circuit parameters as in Fig. 2. When $P_1 = P_2 = P_3$ (squares), F_2 is different from that of the paramagnetic case (diamonds) in contrast to what happens for $\langle I_2\rangle$. At high enough voltages, the cross-correlations are positive in the cases $P_1 = -P_2 = P_3 = 0.6$ (circles) and $P_1 = P_2 = P_3 = 0.6$. Note that the sign of the cross-correlations can be reversed by changing the sign of P_1. The case $-P_1 = P_2 = P_3 = 0.6$ (triangles) illustrates that having a super-Poissonian F_2 is not sufficient to obtain a positive F_{13}.

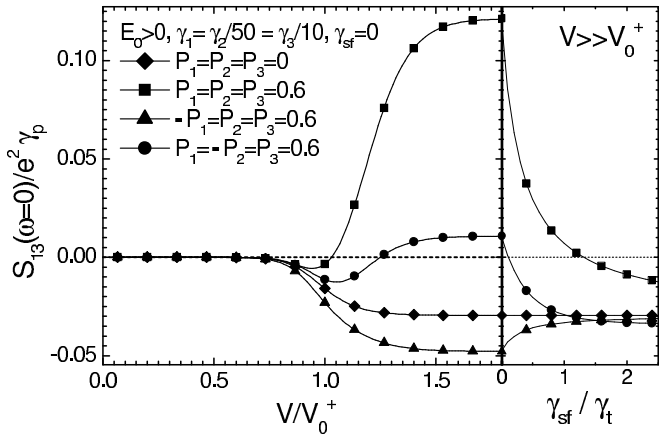

FIG. 4: Zero-frequency cross-correlations $S_{13}(\omega = 0)$ between leads 1 and 3 as a function of the bias voltage V for $\gamma_{sf} = 0$ (left panel) and as a function of γ_{sf} for $V \gg V_0^+$ (right panel). The curves are shown for the same circuit parameters as in Fig. 2. In the paramagnetic case (diamonds), spin-flip scattering has no effect. In the limit of large γ_{sf}, cross-correlations tend to the paramagnetic value.

input current $\langle I_2\rangle$ is shown in the left panel of Fig. 2. This current is exponentially suppressed at low voltages, increases around the voltage V_0^+ and saturates at higher voltages. The width on which $\langle I_2\rangle$ varies is of the order of $\Delta V \sim 10k_BTC/e\,(C_1 + C_3)$. The high-voltage limit of $\langle I_2\rangle$ depends on the polarizations P_i and rates γ_i but not on the capacitances C_i because the tunneling rates saturate at high voltages [see Eq. (2)]. For the paramagnetic case, this limit is

$$e\gamma_p = e\frac{2\gamma_2\gamma_t}{\gamma_t + 2\gamma_2}\ . \tag{28}$$

In this last expression, γ_2 is weighted by a factor 2 to account for both the populations of up and down spins arriving from the input lead. The rate $\gamma_t = \gamma_1 + \gamma_3$ is not weighted by such a factor because there can be only one electron at a time on the dot, which can tunnel to the output leads with the total rate γ_t. For a sample with magnetic contacts, the high-voltage limit of $\langle I_2\rangle$ can be higher or lower than $e\gamma_p$, depending on the parameters considered. Indeed, for $V \gg V_0^+$, we have $I_2(P_1, P_2, P_3) - I_2(0, 0, 0) = e\gamma_p P_{out}\langle\sigma_{dot}\rangle$, where $P_{out} = (P_1\gamma_1 + P_3\gamma_3)/\gamma_t$ is the net output lead polarization, and where $\langle\sigma_{dot}\rangle = \nu(P_2 - P_{out})$ is the average spin of the dot. Here, ν is a positive function of the polarizations, tunneling and scattering rates, which tends to 0 at large γ_{sf}. For $P_1 = P_2 = P_3$, the current is the same as in the paramagnetic case because the populations of spin are matched between the input and the output, thus $\langle\sigma_{dot}\rangle = 0$. Having a saturation current different from the paramagnetic case requires $P_{out} \neq 0$ *and*

$\langle\sigma_{dot}\rangle \neq 0$. When $|P_{out}| > |P_2|$, the high-voltage limit of $\langle I_2\rangle$ is lower than that of the paramagnetic case because the spins in minority at the output block the dot, which leads to a $\langle\sigma_{dot}\rangle$ with the same sign as $-P_{out}$. In this case, $\langle I_2\rangle$ can show negative differential resistance above V_0^+, due to the deblockade of the dot by thermal fluctuations which can send back the blocking spins to electrode 2 for $V \simeq V_0^+$ [30] (see case $P_1 = -P_2 = P_3 = 0.6$ in Fig. 2). Spin-flip scattering modifies the $\langle I_2\rangle(V)$ curve once γ_{sf} is of the order of the tunneling rates. It suppresses spin accumulation and makes the $\langle I_2\rangle(V)$ curve tend to the paramagnetic one.

Figure 3 shows F_2 and F_{13} as a function of V for $\gamma_{sf} = 0$. We also show in Fig. 4 the zero-frequency cross-correlations $S_{13}(\omega = 0)$ because it is the signal measured in practice. Well below V_0^+, $S_{13}(\omega = 0)$ is exponentially suppressed like $\langle I_2\rangle$ because there are very few tunneling events. In this regime, the dot is empty most of the time, and when an electron arrives on the dot, it leaves it with a much higher rate: the electronic transport is limited only by thermally activated tunneling through junction 2. Tunneling events are thus uncorrelated and F_2 is Poissonian, with a unitary plateau following the thermal divergence $2k_BT/eV$ occurring at $V = 0$. For the same reasons, F_{13} displays a zero plateau after a polarization-dependent thermal peak at $V = 0$. Around $V \simeq V_0^+$, F_2, F_{13} and $S_{13}(\omega = 0)$ strongly vary. The high-voltage limit depends on tunneling rates and polarizations. In the paramagnetic case, the high-voltage limit of F_2 lies in the interval $[1/2, 1]$, and that of F_{13} in $[-1/8, 0]$. In the ferromagnetic case, the high-voltage limit of F_2 can be either sub- or super-Poissonian, as already pointed out in the two-terminal case [30]. Spin accumulation is not a necessary condition for having a super-Poissonian F_2, as can be seen for $P_1 = P_2 = P_3$, where $\langle\sigma_{dot}\rangle = 0$. Negative differential resistance is not necessary either (see case $P_1 = P_2 = P_3 = 0.6$ in Figs. 2 and 3). Cross-correlations can be either positive or negative depending on the parameters considered, as shown by Figs. 3 and 4. Interestingly, the sign of cross-correlations can be switched by reversing the magnetization of one contact. The case $P_1 = P_2 = P_3 = 0.6$ of Figs. 3, 4 corresponds to a super-Poissonian F_2 *and* a positive F_{13}. The case $-P_1 = P_2 = P_3 = 0.6$ shows that a super-Poissonian F_2 is not automatically associated with positive output cross-correlations. In this case, the cross-correlations are even more negative than in the paramagnetic case. This will be explained physically in Section III.C.

The effect of spin-flip scattering on $S_{13}(\omega = 0)$ is shown in the right panel of Fig. 4. In the paramagnetic case, spin-flip scattering has no effect on $S_{13}(\omega = 0)$. In the ferromagnetic case, when γ_{sf} is of the order of the tunneling rates, $S_{13}(\omega = 0)$ is modified. In the high-γ_{sf} limit, cross-correlations tend to the paramagnetic case for any value of the polarizations. Thus, strong spin-flip scattering suppresses positive cross-correlations. However, in practice, it is possible to make quantum dots connected to ferromagnetic leads with spin-flip rates much smaller than the tunneling rates [40]. Hence, spin-flip scattering should not be an obstacle for observing positive cross-correlations in the quantum-dot circuit studied here.

B. Zero-frequency results for $E_0 < 0$

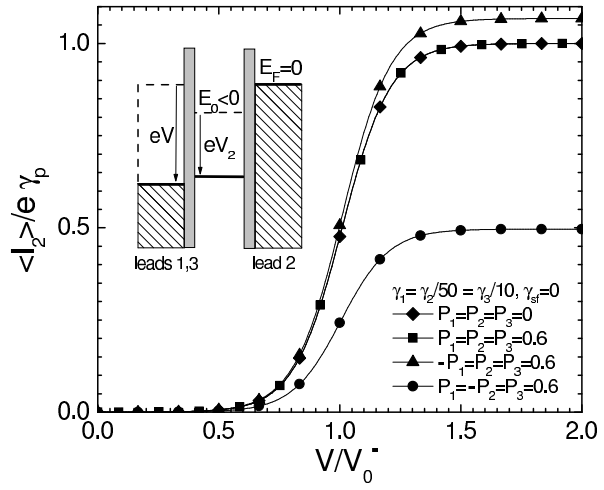

FIG. 5: Current-voltage characteristic of the circuit of Fig. 1 for $E_0 < 0$. The polarizations, tunnel rates, capacitances and reduced temperature $k_BT/|E_0|$ used are the same as in Fig. 2, plotted for $E_0 > 0$. The results differ from the case $E_0 > 0$ only for $V \simeq V_0^-$.

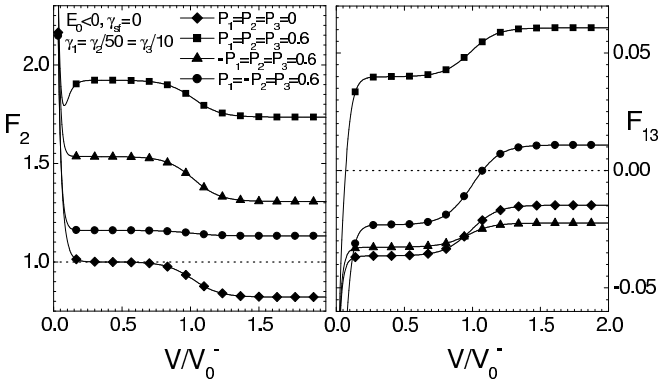

FIG. 6: Input Fano factor F_2 and cross-Fano factor F_{13} as a function of the bias voltage V. The curves are shown for the same circuit parameters as in Fig. 5.

We now discuss the case in which the orbital level E_0 is below the Fermi level of the leads at equilibrium ($E_0 < 0$). First, in the low voltage limit in which very few electrons can flow through the device, $\langle I_2\rangle$ and $S_{13}(\omega = 0)$ exponentially tend to zero like in the case $E_0 > 0$ (Figs. 5 and 7). However, for F_2 and F_{13}, the re-

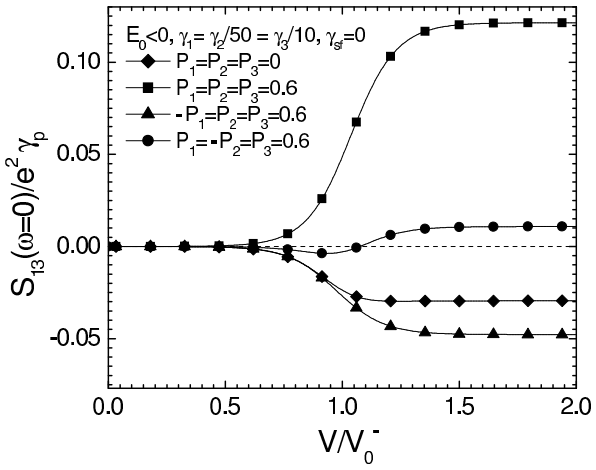

FIG. 7: Zero-frequency current cross-correlations $S_{13}(\omega = 0)$ between leads 1 and 3 as a function of the bias voltage V. The curves are shown for the same circuit parameters as in Fig. 5.

case	$\frac{S_{13}}{e^2\gamma_p}$	$\frac{S_{1\uparrow,3\uparrow}}{e^2\gamma_p}$	$\frac{S_{1\downarrow,3\downarrow}}{e^2\gamma_p}$	$\frac{S_{1\uparrow,3\downarrow}}{e^2\gamma_p}$	$\frac{S_{1\downarrow,3\uparrow}}{e^2\gamma_p}$	$\frac{I_{1\uparrow}}{I_{3\uparrow}}$	$\frac{I_{1\downarrow}}{I_{3\downarrow}}$	n_b
♦	-0.030	-0.007	-0.007	-0.007	-0.007	0.1	0.1	1
■	0.121	0.149	-0.013	-0.007	-0.007	0.1	0.1	4
▲	-0.048	0.026	-0.029	-0.003	-0.042	0.025	0.4	4
•	0.011	0.005	-0.011	0.008	0.008	0.1	0.1	0.25

case	$p_\uparrow$	$p_\downarrow$	p_0	$\gamma_p t_\uparrow$	$\gamma_p t_\downarrow$	$\gamma_p t_0$	$t_b\gamma_p$	$\frac{\gamma_p}{\lvert\lambda^-\rvert}$	$\frac{\gamma_p}{\lvert\lambda^+\rvert}$
♦	0.450	0.450	0.100	0.90	0.90	0.10	1.10	0.09	0.90
■	0.450	0.450	0.099	0.56	2.25	0.10	2.75	0.09	1.46
▲	0.516	0.378	0.106	0.60	1.77	0.10	2.91	0.09	1.31
•	0.056	0.895	0.049	0.563	2.25	0.10	0.26	0.09	0.68

TABLE II: Top: *Zero-frequency* output cross-correlations $S_{13}(\omega = 0)$ and its spin contributions $S_{1\sigma,3\sigma'}(\omega = 0)$, division $I_{1\sigma}/I_{3\sigma}$ of spin currents between leads 1 and 3 and average number n_b of up spins crossing the input junction between two consecutive down spins, for the high-voltage limit $V \gg V_0^{sng(E_0)}$ of the cases studied in Sections III.A and III.B (Figs. 2 to 7). Bottom: Probabilities p_ψ and comparison of the different timescales of the system, for the same parameters (The summation rules (6) and (10) are not exactly verified by the values given in this table because of the limitation in the number of digits).

sults differ (Fig. 6). Above the $2k_BT/eV$ thermal peak, the low voltage plateau of F_2 is always super-Poissonian for $P_{out} \neq 0$. Above a polarization-dependent thermal peak, F_{13} displays a low voltage plateau which is either negative or positive. This features indicate a correlated transfer of charges in spite of the thermally activated limit. In fact, for $V \ll V_0^-$, the dot is occupied most of the time and the electronic transport is limited by thermally activated tunneling through the output junctions 1 and 3. In these conditions, contrarily to what happens for $E_0 > 0$, the polarization of the output leads comes into play even for $V \longrightarrow 0$. Indeed, when $P_{out} \neq 0$, the spins in minority at the output have less chances to leave the dot under the effect of thermal fluctuations. In the intermediate voltage range $V \simeq V_0^-$, the quantities $\langle I_2 \rangle$, F_2, F_{13} and $S_{13}(\omega = 0)$ differ from the case $E_0 > 0$. However, at $V \gg V_0^-$, they take the same values as for $E_0 > 0$ and $V \gg V_0^+$. In this high-voltage limit, the effect of spin flip scattering is identical to that of the case $E_0 > 0$. In particular, the right panels of Figs. 2 and 4 are also valid for $E_0 < 0$.

C. Interpretation of these zero-frequency results: Dynamical Spin-Blockade

In this Section, we provide a physical explanation for the results of Sections III.A and III.B, in the high-voltage limit $V \gg V_0^{sgn(E_0)}$, where the sign of E_0 does not matter. This analysis relies on the evaluation of quantities defined in Section II.A and II.B (Table II), on numerical simulations of the temporal evolution of the spin σ_{dot} of the dot (Fig. 8) and on plots of the correlation functions $\mathcal{C}_{13}(t)$ (Fig. 9).

Let us first focus on the case $P_1 = P_2 = P_3 = 0.6$ (squares in Table II). For these values of lead polarization, up spins are in the majority at the output. Thus, the dwell times of down spins on the dot is longer than that of up spins ($t_\downarrow > t_\uparrow$ in Table II). However, one has $\bar{p}_\downarrow = \bar{p}_\uparrow$ thus $\langle \sigma_{dot} \rangle = 0$. This is because $t_\downarrow > t_\uparrow$ is perfectly compensated by the fact that, due to $P_2 > 0$, up electrons are in the majority in $I_2(t)$. Property $t_\downarrow > t_\uparrow$ suggests that the up spins can flow through the dot only in short time windows where the current transport is not blocked by a down spin. This situation of "dynamical spin-blockade" is responsible for a bunching of the tunneling events associated to the up spins, as confirmed by the numerical simulations of $\sigma_{dot}(t)$ (Fig. 8). The average number of up spins grouped in a "bunch" corresponds to the quantity n_b given in Table II (see [41]). On the one hand, the phenomenon of up-spins bunching is very strong since, here, $n_b = 4$. On the other hand, one can see that the positive sign of $S_{13}(\omega = 0)$ stems from the up-up correlations (see $S_{1\uparrow,3\uparrow}(\omega = 0) > 0$ in Table II). Therefore, one question to answer is whether the positive sign of $S_{13}(\omega = 0)$ can be attributed to this bunching of up-spins tunneling events. For that purpose, we have plotted the correlation function $\mathcal{C}_{13}(t)$ (Fig. 9) and compared it to the characteristic time scales of the electronic transport. The correlation function $\mathcal{C}_{13}(t)$ is negative for times shorter than (approximately) the average delay t_0 between the occupancy of the dot by two consecutive electrons. Then, $\mathcal{C}_{13}(t)$ becomes positive and reaches a maximum at a time comparable to the average delay $t_0 + t_\uparrow$ between the passage of two up spins on

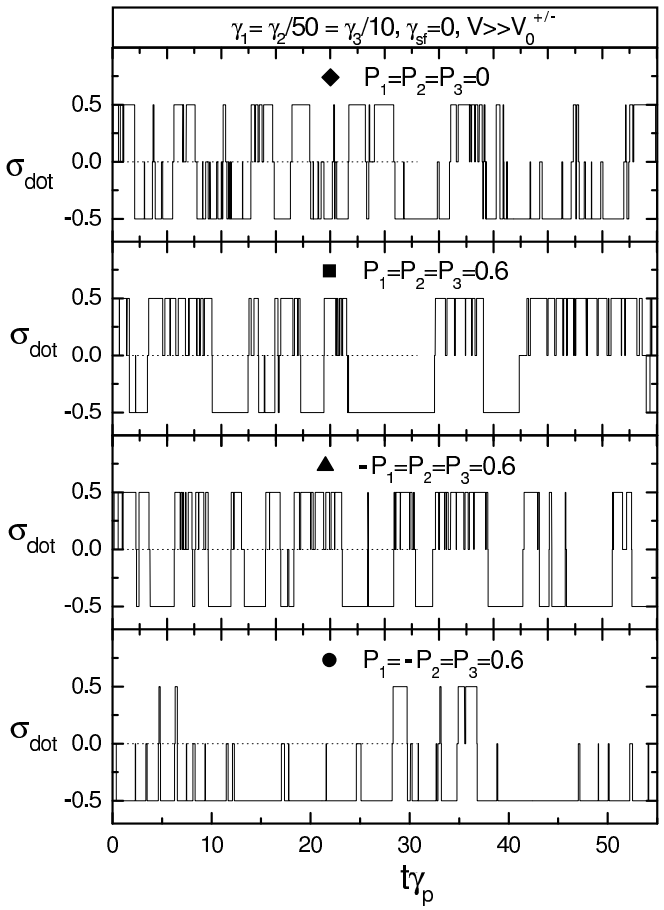

FIG. 8: Numerical simulation of the spin σ_{dot} of the dot as a function of time in the limit $V \gg V_0^{sng(E_0)}$, for the different cases considered in Figs. 2 to 7.

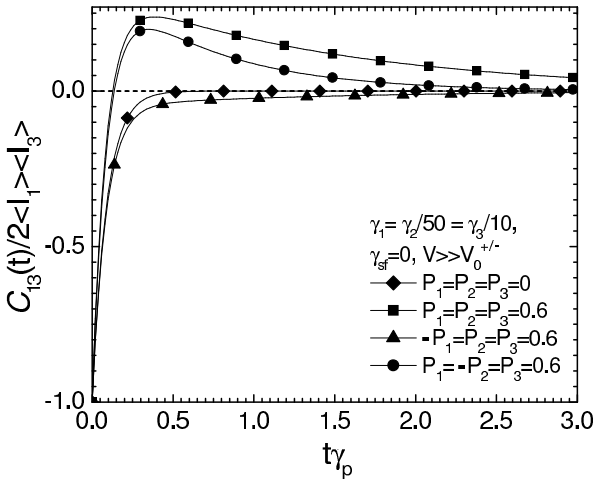

FIG. 9: Time dependence of $\mathcal{C}_{13}(t)$ in the limit $V \gg V_0^{sng(E_0)}$, for the different cases considered in Figs. 2 to 7. Note that $\mathcal{C}_{13}(t)$ is given in units of $-\mathcal{C}_{13}(t=0) = 2\langle I_1\rangle\langle I_3\rangle$, which depends on the polarization values.

the dot. Eventually, $\mathcal{C}_{13}(t)$ is strongly decreased at times of the order of the average duration t_b of the "bunch" of spins. Hence, the time-dependence of $\mathcal{C}_{13}(t)$ allows us to attribute the positive value of $S_{13}(\omega=0)$ to the bunching of tunneling events caused by dynamical spin-blockade. The same reasoning can be made to explain the super-Poissonian value of F_2 (data not shown).

In the case $-P_1 = P_2 = P_3 = 0.6$ (triangles in Table II), the temporal evolution of σ_{dot} (see Fig. 8) is qualitatively similar to that of the case $P_1 = P_2 = P_3 = 0.6$, thus up-up correlations caused by dynamical spin-blockade lead again to a super-Poissonian F_2. However, less up electrons flow through lead 1 than in the previous case because the polarization P_1 has been reversed (see $I_{1\uparrow}/I_{3\uparrow}$ in Table II). Hence, the positive term $S_{1\uparrow,3\uparrow}(\omega=0)$ is not large enough to lead to a positive $S_{13}(\omega=0)$.

In the case $P_1 = -P_2 = P_3 = 0.6$ (circles in Table II), there is still dynamical spin-blockade, as shown by $t_\downarrow > t_\uparrow$ in Table II. This dynamical spin-blockade induces again a bunching of the tunneling of up spins (see $S_{1\uparrow,3\uparrow}(\omega=0) > 0$ in Table II). However, the up-up correlations are much weaker than in the $P_1 = P_2 = P_3 = 0.6$ case due to the minority of up spins at the input. Another positive contribution to the cross-correlations stems from the up-down terms (see $S_{1\sigma,3-\sigma}(\omega=0) > 0$ in Table II). In fact, since the average number $n_b = 0.25$ of up spins passing consecutively through the dot is very low [41], we have $t_b < t_\downarrow$. Then, each up spin is positively correlated to the first down spin preceding him (see Fig. 9). As a result, dynamical spin-blockade now produces a bunching of tunneling events responsible for up-up *and* up-down correlations. The correlation function $\mathcal{C}_{13}(t)$ differs from that of the case $P_1 = P_2 = P_3 = 0.6$ in the sense that it decreases more quickly after its maximum, due to the smaller value of t_b. However, contrarily to the case $P_1 = P_2 = P_3 = 0.6$, the decay time of $\mathcal{C}_{13}(t)$ is much larger than t_b, due to large fluctuations in the number of spins per bunch with respect to $n_b = 0.25$ (Fig. 8).

In conclusion, we have seen that in all the cases treated here, the super-Poissonian value of F_2 and the positive sign of F_{13} can be explained from the dynamical spin-blockade mechanism which induces a bunching of the tunneling events.

D. Effect of tunneling asymmetry

We now address the problem of how to choose parameters that favor the observation of positive cross-correlations in the ferromagnetic case treated here. First, from Section II.C, finite lead polarizations are necessary. However, it is possible to get positive cross-correlations even if $P_2 = 0$, provided the output of the device is sufficiently polarized. For instance, in the high-voltage limit $V \gg V_0^{sgn(E_0)}$, choosing $P_1 = P_3$, $P_2 = 0$ and $\gamma_{sf} = 0$

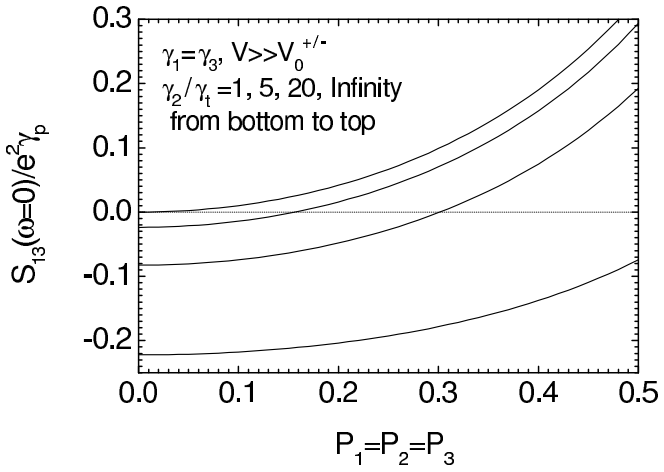

FIG. 10: Influence of the asymmetry between γ_2 and γ_t on $S_{13}(\omega=0)$, for $V \gg V_0^{sgn(E_0)}$, $P_1 = P_3 = P_3$, $\gamma_1 = \gamma_3$ and $\gamma_{sf} = 0$. According to (30), for these parameters, $S_{13}(\omega=0)$ is always positive for high enough values of P_1. Large ratios $\gamma_2/\widetilde{\gamma}$ favor positive cross-correlations by extending the positivity domain to lower polarization values. In the limit $\gamma_2 \gg \gamma_t$, the curve tends to $S_{13}(\omega=0) = 4\gamma_1\gamma_3 P_1^2 e^2/\gamma_t\left(1-P_1^2\right)$.

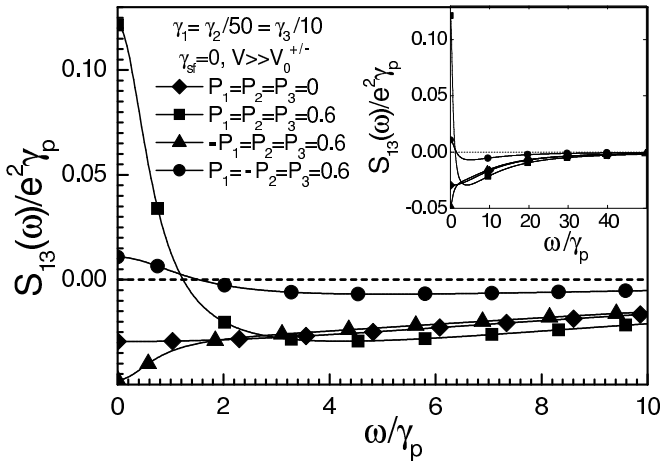

FIG. 11: Frequency dependence of $S_{13}(\omega)$ in the high-voltage limit $V \gg V_0^{sgn(E_0)}$, for the different cases considered in Figs. 2 to 7. The inset shows the same data for a larger frequency scale.

leads to

$$S_{13}(\omega=0) = \frac{16e^2\gamma_1\gamma_2^2\gamma_3\left(1-P_1^2\right)\left[P_1^2(2\gamma_2+\gamma_t)-\gamma_t\right]}{\gamma_t[2\gamma_2+(1-P_1^2)\gamma_t]^3} . \tag{29}$$

In this limit, the current $\langle I_2\rangle$ *is not spin polarized*, i.e. $\langle I_{2,\uparrow}\rangle = \langle I_{2,\downarrow}\rangle$, because up and down spins have the same probability to enter the dot, regardless of what happens at the output. The case where the three electrodes are polarized in the same direction leads to a higher positive $S_{13}(\omega=0)$ because spin accumulation is suppressed ($\langle\sigma_{dot}\rangle = 0$). Indeed, in the high-voltage limit, choosing $P_1 = P_2 = P_3$ and $\gamma_{sf} = 0$ leads to

$$S_{13}(\omega=0) = \frac{16e^2\gamma_1\gamma_2^2\gamma_3[P_1^2(2\gamma_2+\gamma_t)-\gamma_t]}{\gamma_t(2\gamma_2+\gamma_t)^3(1-P_1^2)} . \tag{30}$$

The asymmetry between the tunneling rates γ_i has a strong influence on the cross-correlations. From (30), the case of symmetric output junctions, i.e. $\gamma_1 = \gamma_3$, is the most favorable configuration for getting a large $S_{13}(\omega=0) > 0$ when $P_1 = P_2 = P_3$ [42]. In addition, choosing large values of γ_2/γ_t decreases $\bar{p}_0$, which allows to extend the domain of positive cross-correlations to smaller values of polarizations (Fig. 10). This is important because ferromagnetic materials are usually not fully polarized (see for instance [43]).

E. Finite frequency results

Equation (16) gives the frequency dependence of $S_{13}(\omega)$. The spectrum $S_{13}(\omega)$ deviates from its zero frequency limit for $\omega \gtrsim |\lambda_+|$. In the case $S_{13}(\omega=0) > 0$, properties $|\lambda_+| < |\lambda_-|$, $\mathcal{C}_{13}(t=0) < 0$, $S_{13}^{+} > 0$ and $S_{13}^{-} < 0$ (see Section II.C) imply that cross-correlations always turn to negative when ω increases. Then, for frequencies larger than $|\lambda_-|$, $S_{13}(\omega)$ tends to zero (see Fig. 11).

Eq. (27) gives the expression of the total current cross-correlations $S_{13}^{tot}(\omega)$ measured in practice, including the contribution of screening currents. The spectrum $S_{13}^{tot}(\omega)$ differs from $S_{13}(\omega)$ only for $\omega \gtrsim |\lambda_+|$. At large frequencies $\omega \gg |\lambda_-|$, $S_{13}^{tot}(\omega)$ become a linear mixture of the Schottky noises through the three junctions. If we furthermore assume $V \gg V_0^{sgn(E_0)}$, current conservation leads to

$$\frac{S_{13}^{tot}(\omega)}{2e} = \frac{I_1C_3}{C^2}(C_1-C_2-C_3)+\frac{I_3C_1}{C^2}(C_3-C_1-C_2) .$$

This limit depends on the values of C_i considered, in contrast to what happens for $S_{ij}(\omega)$. It can be positive as well as negative depending on the values of parameters. For $P_1 = P_2 = P_3 = 0.6$, $\gamma_1 = \gamma_2/50 = \gamma_3/10$, $C_1 = C_2 = C_3$ and $V \gg V_0^{sgn(E_0)}$, one has a cross-over from positive to negative cross-correlations as ω increases ($S_{13}^{tot}(\omega=0)/e^2\gamma_p \simeq +0.121$ and $S_{13}^{tot}(\omega \gg |\lambda_-|)/e^2\gamma_p \simeq -0.222$). But the opposite situation is also possible. For instance, with $P_1 = P_2 = P_3 = 0$, $\gamma_1 = \gamma_2/50 = \gamma_3/10$, $C_1 = C_2 = C_3/5$ and $V \gg V_0^{sgn(E_0)}$, one has $S_{13}^{tot}(\omega=0)/e^2\gamma_p \simeq -0.030 < 0$ and $S_{13}^{tot}(\omega \gg |\lambda_-|)/e^2\gamma_p \simeq +0.019 > 0$. For other positive cross-correlations due to screening currents, see [25]. We recall that the results shown in this Section are valid if the Markovian approximation holds, i.e. here $\hbar\omega < \min_i(|E_0 - eV_i|)$ [38]. The results for the correlations of $I_j^{tot}(t)$ are furthermore valid only for ω larger than the characteristic frequencies associated to the charging of the capacitors (see Section

II.E).

F. Comments

In spite of the large variety of proposals for getting positive cross-correlations, this effect has not been observed experimentally yet. We believe that the mechanism proposed in Section III can be implemented with present techniques. For $\gamma_1 = \gamma_2/10 = \gamma_3$, the polarizations $P_1 = P_2 = P_3 = 0.4$ typical for Co [43] lead to positive cross-correlations of the order of $S_{13}/e^2\gamma_{tot} \simeq 0.08$. With $\gamma_p \simeq 5$ GHz, this corresponds to a current noise level of $10^{-29}\mathrm{A}^2\mathrm{s}$. The maximum differential conductance of the sample depends on temperature: $d\langle I_2\rangle/dV \sim e^2\gamma_p(C_1+C_3)/5k_BTC$. Assuming that $T = 20$ mK and $C_1 = C_2 = C_3$, one obtains $(d\langle I_2\rangle/dV)^{-1} \sim h/e^2$. This leads to a voltage noise level measurable with existing voltage noise-amplification techniques [29, 44].

One difficulty of this experiment is connecting three leads to a very small structure. We believe that a multiwall carbon nanotube (MWNT) contacted by ferromagnetic leads could be an interesting candidate for implementing a three-terminal device. The question of whether a MWNT splits into two quantum dots when three contacts are evaporated on top it is still open. However, given that the intrinsic level spacing of a MWNT connected to two leads seems to be determined by its total length rather than by the separation between the leads [45], a three-terminal quantum dot structure seems feasible. In addition, it has been demonstrated experimentally that contacting ferromagnetic leads to a MWNT is possible [46].

Interestingly, a different mechanism, proposed by Sauret and Feinberg, can also lead to positive current cross-correlations in a quantum-dot circuit connected to ferromagnetic leads [47]. This work also considers current transport through one single orbital of the dot. For certain bias voltages large enough to allow a double occupation of this orbital, the Pauli principle induces positive correlations between up and down spins. This so-called mechanism of "opposite-spin bunching" is antagonist to our mechanism of dynamical spin-blockade which requires that the orbital can be only singly occupied. However, with both mechanisms, positive cross-correlations can be obtained only when the two spin channels do not transport current independently, i.e. when charging effects are relevant [48]. We point out that in the three-terminal geometry of Figure (1), the opposite-spin bunching proposed by Sauret *et al.* allows to get positive output cross-correlations in spite of a sub-Poissonian input Fano factor. This feature, added to our findings, shows that positive output cross-correlations and a super-Poissonian input Fano factor can be obtained *separately* for a quantum dot connected to ferromagnetic leads. Nevertheless, the opposite-spin bunching proposed by Sauret *et al.* can lead to positive cross-correlations between the total currents through leads 1 and 3 only when the output leads are *strongly* polarized in opposite directions, in order to filter the weak up-down positive cross-correlations induced by this effect. In practice, this is very difficult to achieve with usual ferromagnetic materials [43].

Note that the dynamical spin-blockade studied in this article is unrelated with another mechanism called "spin-blockade", observed in many semiconductor quantum dots experiments (see [49] and references therein). This other spin-blockade refers to the suppression of peaks expected in the I-V characteristics of a quantum dot for independent single electron states, but not observed due to quantum mechanical spin selection rules.

IV. ONE-ORBITAL QUANTUM DOT IN A MAGNETIC FIELD, CONNECTED TO THREE PARAMAGNETIC LEADS

In view of the experimental difficulties for connecting ferromagnetic leads to semiconductor quantum dots [50], the question of whether it is possible to obtain positive cross-correlations without using ferromagnetic leads is of great interest. We thus consider in Sections IV.A and IV.B the one-orbital case introduced in section II, with $P_1 = P_2 = P_3 = 0$ and $B \neq 0$.

At $B \neq 0$, two resonances are expected a priori in the voltage characteristics, for $V \simeq V_\uparrow^{sgn(E_0)}$ and $V \simeq V_\downarrow^{sgn(E_0)}$. The limit $V \gg V_{\max}^{sgn(E_0)}$ and $\gamma_{sf} = 0$ is the same as in the $B = 0$ case because the tunneling rates saturate at high voltages. In particular, from Eqs. (25), (28) and (30), we have in this limit

$$F_2 = \frac{4\gamma_2^2+\gamma_t^2}{(\gamma_t+2\gamma_2)^2}$$
$$F_{13} = -\frac{4\gamma_1\gamma_2\gamma_3}{\gamma_t(\gamma_t+2\gamma_2)^2}\ . \qquad (31)$$

This means that here, a super-Poissonian F_2 and positive cross-correlations can appear only at lower voltages, for which the cases $E_0 > 0$ and $E_0 < 0$ differ significantly. Note that due to $P_1 = P_2 = P_3 = 0$, one obtains from Eqs. (4) and (12):

$$S_{13} = \frac{\gamma_1\gamma_3}{\gamma_t}\mathcal{F}(\frac{\gamma_2}{\gamma_t}, \frac{\gamma_{\uparrow\downarrow}}{\gamma_t}, \frac{\gamma_{\downarrow\uparrow}}{\gamma_t}, \frac{E_0}{T}, \frac{V}{T}, \frac{B}{T}) \qquad (32)$$

According to (32), for a constant value of γ_t, $\gamma_1 = \gamma_3$ allows to maximize $|S_{13}|$. Therefore, in this section, we will plot curves for $\gamma_1 = \gamma_3$.

A. Zero-frequency results for $E_0 > 0$

We first briefly comment the case in which the two Zeeman sublevels are above the Fermi energy at equilib-

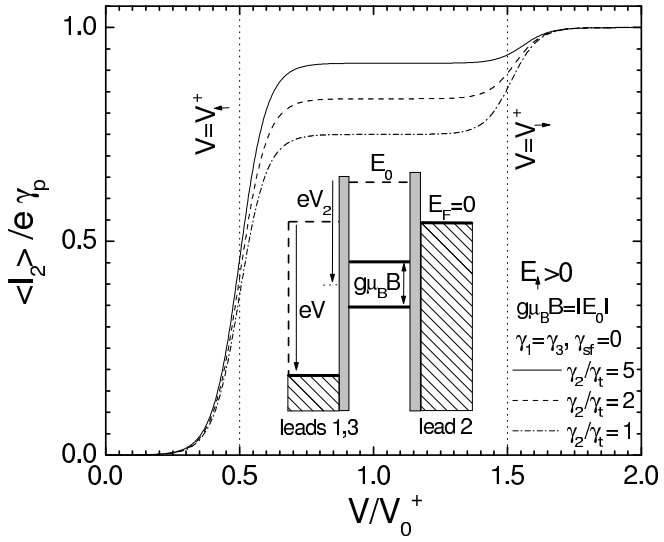

FIG. 12: Average current $\langle I_2\rangle$ as a function of the bias voltage V for $E_0 > 0$, $P_1 = P_2 = P_3 = 0$, $C_1 = C_2 = C_3$, $\gamma_1 = \gamma_3$, $k_BT/|E_0| = 0.05$, $g\mu_B B/|E_0| = 1$, and different values of γ_2/γ_t. These curves display two steps, for $V \simeq V_\uparrow^+$ and $V \simeq V_\downarrow^+$. The inset shows electrochemical potentials in the circuit.

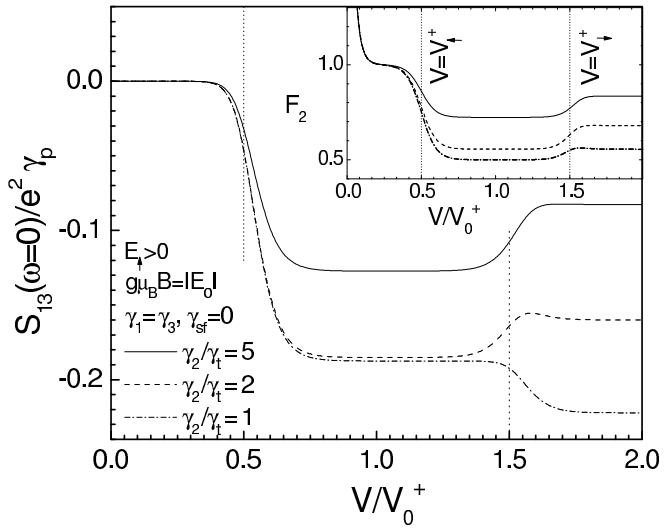

FIG. 13: Zero-frequency current cross-correlations $S_{13}(\omega = 0)$ between leads 1 and 3 as a function of the bias voltage V for the same circuit parameters as in Fig. 12. Inset: Fano factor F_2. These curves display two steps, for $V \simeq V_\uparrow^+$ and $V \simeq V_\downarrow^+$. Above the thermal peak, for $\gamma_{sf} = 0$, one has $F_2 \leq 1$ and $S_{13}(\omega = 0) \leq 0$ for any values of the parameters.

rium (*i. e.* $E_{\uparrow(\downarrow)} > 0$). The current and noise voltage-characteristics obtained in this situation were already discussed in Ref. [51] for the two-terminal case. Like in III.A, for $V < V_\uparrow^+$, $\langle I_2\rangle$ and $S_{13}(\omega = 0)$ are exponentially small and F_2 is Poissonian with a thermal peak at $V \to 0$, followed by a unitary plateau (Figs. 12 and 13). Then, the curves $\langle I_2\rangle$, F_2 and $S_{13}(\omega = 0)$ show two steps corresponding to $V \simeq V_\uparrow^+$ and then $V \simeq V_\downarrow^+$. We have verified analytically that, above the thermal peak, for $\gamma_{sf} = 0$, one has $F_2 \leq 1$ and $F_{13} \leq 0$ for any values of the parameters. For $V < V_\downarrow^+$, the current $\langle I_2\rangle$ is spin polarized, an effect which allows to do spin filtering with a nearly 100% efficiency [52, 53].

B. Zero-frequency results for $E_0 < 0$

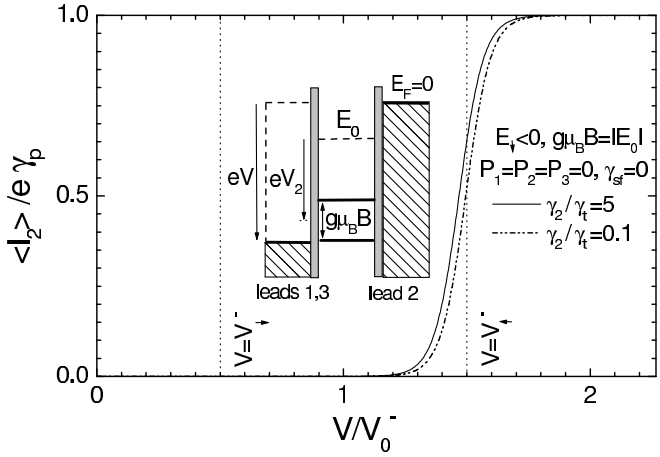

FIG. 14: Current-voltage characteristic of the circuit of Fig. 1 for $E_0 < 0$, $P_1 = P_2 = P_3 = 0$, $C_1 = C_2 = C_3$, $\gamma_1 = \gamma_3$, $k_BT/|E_0| = 0.05$, $g\mu_B B/|E_0| = 1$, and different values of the asymmetry γ_2/γ_t between the input and the output. These curves display only one step, for $V \simeq V_\uparrow^-$. The inset shows the electrochemical potentials in the circuit.

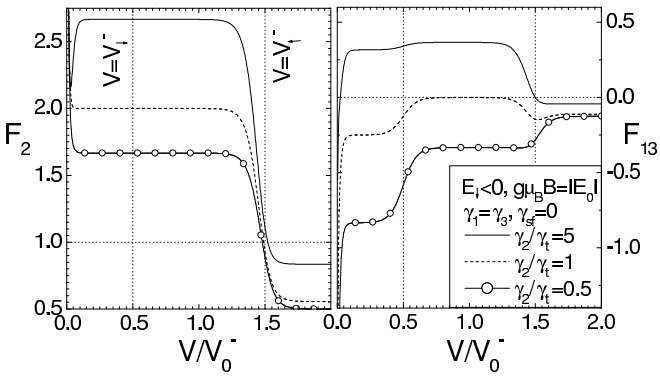

FIG. 15: Input Fano factor F_2 (left panel) and output cross-Fano factor F_{13} (right panel) as a function of the bias voltage V, for the same circuit parameters as in Fig. 14. In all curves $\gamma_{sf} = 0$. The Fano factor F_2 shows only one step for $V \simeq V_\uparrow^-$ whereas F_{13} shows two steps, for $V \simeq V_\downarrow^-$ and $V \simeq V_\uparrow^-$. F_2 can be super-Poissonian and F_{13} positive for certain values of γ_2/γ_t and V (see text).

Below, we focus on the case in which the two Zeeman sublevels are below the Fermi energy at equilibrium (i.e. $E_{\uparrow(\downarrow)} < 0$). To our knowledge, the current noise in this configuration has never been studied

before, even for a two-terminal device. We will first study analytically what happens above the thermal peak, i.e. $eV \gg k_BT$. In this limit, one can write the tunneling rates as $\Gamma^+_{2\sigma} = \gamma_2$, $\Gamma^-_{2\sigma} = 0$, $\Gamma^-_{1(3)\uparrow} = x\gamma_{1(3)}$, $\Gamma^+_{1(3)\uparrow} = (1-x)\gamma_{1(3)}$, $\Gamma^-_{1(3)\downarrow} = y\gamma_{1(3)}$, and $\Gamma^+_{1(3)\downarrow} = (1-y)\gamma_{1(3)}$, where $x = 1/(1+\exp[-(E_\uparrow - eV_1)/k_BT])$ and $y = 1/(1+\exp[-(E_\downarrow - eV_1)/k_BT])$. The hypothesis $B > 0$ implies that $x < y$. First, for $V < V^-_\downarrow$, we have $x \to 0$ and $y \to 0$. Then, the parameters x and y go from 0 to 1 while the voltage increases. For $V = V^-_\downarrow$ i.e. $y = 1/2$, the upper Zeeman sublevel is at resonance with the Fermi level of the output leads 1 and 3. Then, for $V = V^-_\uparrow$ i.e. $x = 1/2$, the lower Zeeman sublevel is at resonance with the outputs, as represented by the level diagram in Fig. 14.

The assumptions made on the rates lead to

$$F_{13} = \frac{\gamma_1\gamma_3}{\gamma_2\gamma_t^2}\left[\gamma_2\left(F_2 - 1\right) + \gamma_t(x+y-2)\right] \ . \qquad (33)$$

In Section II, we have shown that relation (25) between F_2 and F_{13} is always valid at high voltages (i.e $x, y \sim 1$ here) for the single-orbital problem with $P_1 = P_2 = P_3$. But this demonstration does not take into account the symmetries that the problem takes for certain particular cases. Here, from (33), $P_1 = P_2 = P_3 = 0$ implies that property (25) is also valid at any V above the thermal peak when $\gamma_2 \gg \gamma_t$.

The inequality $t_\downarrow = 1/y\gamma_t \neq t_\uparrow = 1/x\gamma_t$ for $x \neq y$ suggests the possibility of obtaining again dynamical spin-blockade. To study the situation accurately, we will consider the simple limit $k_BT \ll g\mu_BB$, i.e. the up-spins channel starts to conduct for voltages such that down spin can flow only from the right to the left. This means that for the first voltage transition $V \simeq V^-_\downarrow$ (i.e. $y \simeq 1/2$), we have $x \ll 1$ and it is enough to consider low order developments of $\langle I_2\rangle$, F_2, and F_{13} with respect to x:

$$\langle I_2\rangle = \frac{2e\gamma_2\gamma_t x}{\tilde{\gamma} + \gamma_2} + o(x)^2 \ , \qquad (34)$$

$$F_2 = \frac{\gamma_t + 3\gamma_2}{\gamma_t + \gamma_2} + o(x) \qquad (35)$$

and

$$F_{13} = \frac{\gamma_1\gamma_3\left[(2\gamma_2^2 - \gamma_t\left(\gamma_t + \gamma_2\right)(2-y)\right]}{\left(\gamma_t + \gamma_2\right)\gamma_2\gamma_t^2} + o(x) \qquad (36)$$

for $\gamma_{sf} = 0$. Transport through the upper level is energetically allowed for $y > 1/2$. However, since we have assumed $x \ll 1$, from Eq. (34), $\langle I_2\rangle$ remains very small throughout the $V \simeq V^-_\downarrow$ transition: the dot is blocked by up spins, thus down spins cannot cross the dot. Even if the current is very low, this leads to dynamical spin-blockade and thus to a super-Poissonian F_2, except in the limit $\gamma_t \gg \gamma_2$ [see Eq. (35)]. Accordingly, F_{13} can be positive for certain tunneling rate asymmetries [Eq. (36)]. The factor F_{13} shows a step around $V \simeq V^-_\downarrow$, due to the y dependence in Eq. (36), whereas F_2 is constant throughout the $V \simeq V^-_\downarrow$ transition. This implies a redistribution of the zero-frequency noise between $S_{11}(\omega=0)$, $S_{33}(\omega=0)$ and $S_{13}(\omega=0)$ when the threshold $V = V^-_\downarrow$ is crossed [see (23)]. The absence of step for F_2 can be attributed to the unidirectionality of tunneling through junction 2. Indeed, $x \to 0$ means that F_2 depends only on p_0 and $G_{0,\uparrow(\downarrow)}$ [see (7) and (12)]. Now, for $V \simeq V^-_\downarrow$, the contribution of these terms is independent of y (and thus on V) at first order in x, because $\bar{p}_0$ and $G_{0,\uparrow(\downarrow)}$ are already forced to very low values due to the $x \to 0$ hypothesis. On the contrary, F_{13} also depends on $\bar{p}_{\uparrow,\downarrow}$ and $G_{\sigma,0}$ with $\sigma \in \{\uparrow, \downarrow, 0\}$. For $x \to 0$, these last terms depend strongly on y.

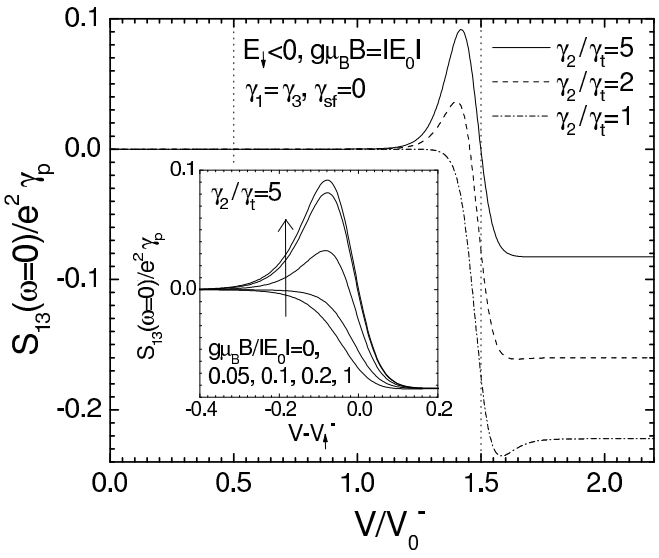

FIG. 16: Zero-frequency current cross-correlations $S_{13}(\omega=0)$ between leads 1 and 3 as a function of the bias voltage V, for the same circuit parameters as in Fig. 14 and different values of junction asymmetry. The inset shows the effect of a magnetic field B for $\gamma_2/\gamma_t = 5$ and $\gamma_{sf} = 0$.

For $k_BT \ll g\mu_BB$, the second possible voltage transition $V \simeq V^-_\uparrow$ (i.e. $x \simeq 1/2$) can be described by taking the limit $y = 1$ where

$$\langle I_2\rangle = \frac{2ex\gamma_2\gamma_t}{\gamma_t + \gamma_2(1+x)} \ , \qquad (37)$$

$$F_2 = 1 + \frac{2\gamma_2\left(\gamma_t(1-3x) + (1-x)^2\gamma_2\right)}{\left(\gamma_t + \gamma_2(1+x)\right)^2} \qquad (38)$$

and

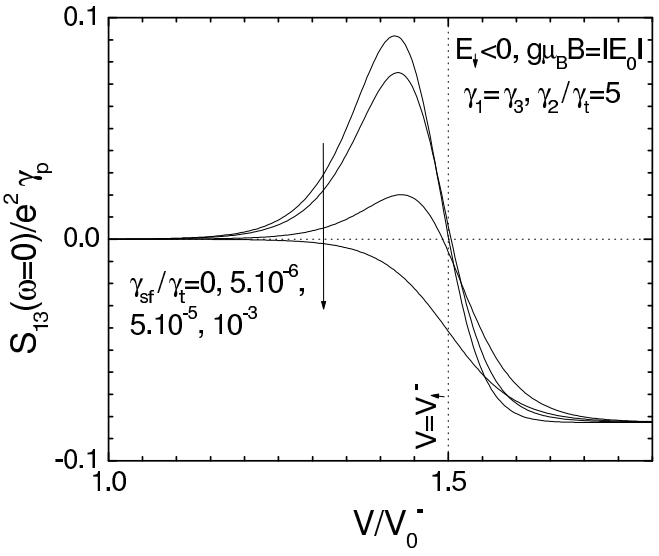

FIG. 17: Effect of spin flip-scattering on the current cross-correlations between leads 1 and 3 for the same circuit parameters as in Fig. 16 and $\gamma_2/\gamma_t = 5$.

$$F_{13} = \frac{\gamma_1\gamma_3}{\gamma_t^2}\frac{1}{\gamma_2(\gamma_t+(1+x)\gamma_2)^2}[\\ 2(1-x)^2\gamma_2^3 + (1-7x+x^2+x^3)\gamma_2^2\gamma_t \\ -2(1-x^2)\gamma_2\gamma_t^2 - (1-x)\gamma_t^3] \quad (39)$$

for $\gamma_{sf} = 0$. Around $V \simeq V_\uparrow^-$, the blockade of the dot by up spins is partially lifted and transport through both levels is allowed. The average input current $\langle I_2\rangle$ thus increases with voltage (i.e. with x) [see (37)]. On the opposite of what happens in IV.A, the average current $\langle I_2\rangle$ is *not spin-polarized* because up and down spin have the same probability to enter the dot. The factors F_2 and F_{13} both show a step through the $V \simeq V_\uparrow^-$ transition (as indicated by their x-dependency) and tend at high voltages to the usual sub-Poissonian values.

We now turn to the discussion of the general results displayed in Figs. (14-17), obtained from an exact treatment of the full Master equation. Fig. 14 shows the full voltage dependence of $\langle I_2\rangle$. As expected from (34) and (37), this current shows a single step at $V \simeq V_\uparrow^-$, an effect observed experimentally [54–56]. The width on which $\langle I_2\rangle$ varies is of the order of $\Delta V \sim 10k_BTC/eC_2$, whereas the position of the step varies only slightly with the asymmetry of the junctions (the maximal variation is about $\Delta V' \sim 0.7k_BTC/eC_2$).

The left panel of Fig. 15 shows the voltage dependence of F_2. The low-voltage divergence of F_2 is again a result of the dominating thermal noise in the limit $k_BT \gtrsim eV$. As expected from (35) and (38), F_2 shows one single step at $V \simeq V_\uparrow^-$, surrounded by two plateaus, and the low voltage plateau of F_2 is super-Poissonian because $t_\downarrow > t_\uparrow$ induces dynamical spin blockade (except in the limit $\gamma_t \gg \gamma_2$). The right panel of Fig. 15 shows the voltage dependence of F_{13}. As expected from (36) and (39), F_{13} shows two steps at $V \simeq V_\downarrow^-$ and then $V \simeq V_\uparrow^-$, and F_{13} can be positive at low voltages, due again to $t_\downarrow > t_\uparrow$. The first plateau displayed by F_{13} is positive for $\gamma_2 > \gamma_t\left(1+\sqrt{5}\right)/2$ and the second for $\gamma_2 > \gamma_t$, as can be seen from (36). The high-voltage plateau of F_{13} is negative because $t_\uparrow$ and $t_\downarrow$ tend to the same value. Note that the case $\gamma_2/\gamma_t = 1/2$ and $V_\downarrow^- < V < V_\uparrow^-$ is one more illustration that it is possible to have F_2 super-Poissonian and $F_{13} < 0$.

It is also interesting to look at $S_{13}(\omega = 0)$ which is the signal measured in practice (Fig. 16). Like $\langle I_2\rangle$, the cross-correlations $S_{13}(\omega = 0)$ are exponentially small for $V \simeq V_\downarrow^-$, thus the first voltage step of F_{13} is not visible on the scale of Fig. 16. Cross-correlations have a significant variation around the voltage $V \simeq V_\uparrow^-$, for which the blockade of the dot by up spins is partially lifted. When $\gamma_2 > \gamma_t$, this variation consists of a positive peak consistent with the positive plateau found for F_{13}. The maximum positive $S_{13}(\omega = 0)$ obtained at this peak is of the same order as the maximum $S_{13}(\omega = 0)$ predicted in the ferromagnetic case for comparable junction asymmetries (see Section III.F). Note that the height of the peak is independent of temperature as long as (1) is fulfilled, whereas its width, which is approximately ΔV, depends on temperature. At high voltages $S_{13}(\omega = 0)$ is always negative, in agreement with the behavior of F_{13}.

Since the positive cross-correlations found in this work are due to dynamical spin-blockade, we expect a strong dependence on the magnetic field. The inset of Fig. 16 shows the voltage dependence of $S_{13}(\omega = 0)$ around the step $V_\uparrow^-$, for a fixed temperature, a tunneling asymmetry $\gamma_2/\gamma_t = 5$, and various magnetic fields. The amplitude of the positive peak first increases with B and then saturates once the Zeeman splitting of the levels is much larger than the thermal smearing of the resonances (i.e. $g\mu_B B \geq 8k_BT$). The peak then simply shifts to larger bias voltages V while B increases. Fig. 17 shows the effect of spin-flip scattering on the cross-correlations. Spin flips modify the positive peak of $S_{13}(\omega = 0)$ when $\Gamma_{\uparrow\downarrow} = \gamma_{sf}\exp(g\mu_B B/2k_BT) \sim \gamma_i$, see Eq. (4). As expected, a strong spin-flip scattering suppresses all spin-effects and turns the positive cross-correlations to negative. It is thus preferable to use a B not larger than $8k_BT$ when spin flip scattering is critical.

C. Comments

There is a strong qualitative difference between the ferromagnetic case of Section III and the $B \neq 0$ case of Section IV: in Section IV we have obtained positive cross-correlations in the form of a peak around a resonance voltage whereas in Section III, positive cross-correlations

reach their maximum above the resonance voltage.

In practice, we can imagine to tune the bias voltage V such that different orbital levels will transport current successively while the gate voltage of the dot is swept, leading to an effective E_0 oscillating between positive and negative values. In this situation, the results of Sections IV.A and V.B indicate the possibility of having the sign of $S_{13}(\omega = 0)$ which oscillates with the gate voltage.

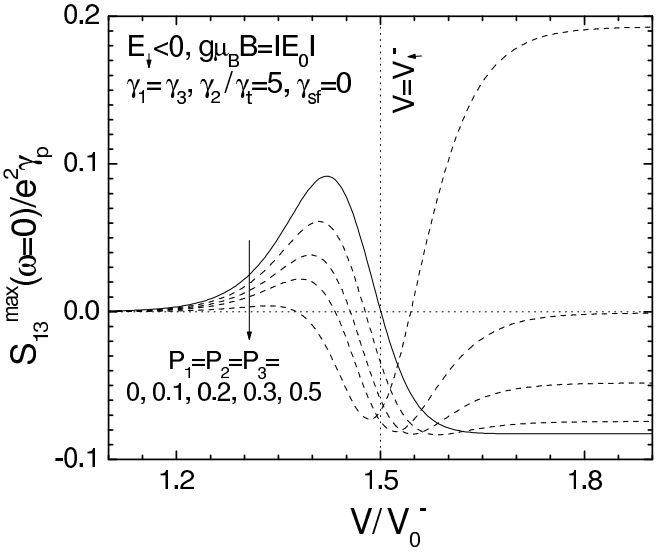

FIG. 18: Zero-frequency current cross-correlations between leads 1 and 3 as a function of the bias voltage for the same circuit parameters as in Fig. 16, $\gamma_2/\gamma_t = 5$ and $\gamma_{sf} = 0$. The full line corresponds to the case $P_1 = P_2 = P_3 = 0$ shown in Fig. 16 and the dashed lines to finite values of $P_1 = P_2 = P_3$.

MWNTs could be possible candidates for observing this effect. However, lateral semiconductor quantum dots seem even more attractive. The fabrication technology of lateral semiconductor quantum dots allows to engineer more than two leads just by adjusting a lithography pattern (see for instance [39]). Another advantage of these structures is that the asymmetry of the tunnel junctions, which is very critical for getting dynamical spin-blockade, can be controlled just by changing the voltage of the gates delimiting them. In addition, it has been shown that the spin-flip rate can be very low in semiconductor quantum dots [56, 57]. However, implementing the model of Section IV requires that the leads can be considered as unpolarized, which is not obvious in these systems if the magnetic field is not applied locally to the dot but to the whole circuit. In certain cases, the magnetic field can induce a significant spin polarization at the edges of the two-dimensional electron gas, leading to different net tunneling rates $\gamma_{j,\uparrow}$ and $\gamma_{j,\downarrow}$ for up and down spins [53, 58, 59]. In an extremely simplified approach, we have taken this effect into account with finite polarizations $P_1 = P_2 = P_3$ with the same sign as B (see Fig. 18). The positive peak of $S_{13}(\omega = 0)$ is suppressed while P_1 increases because the tunneling rates of spins which blocked the dot for $P_1 = P_2 = P_3 = 0$ increase. However, this positive peak is replaced by a high-voltage positive limit simply identical to that of Section III for the corresponding polarizations. Note that for semiconductor quantum dots in the few electron regime, the time evolution of $|\sigma_{dot}|$ can be measured by coupling the dot to a single electron transistor or a quantum point contact [60–63]. In the high-voltage limit where current transport is unidirectional, studying the statistics of $|\sigma_{dot}(t)|$ would give a direct access to $S_{22}(\omega)$ for currents too low to be measured with standard techniques.

V. TWO-ORBITAL SPIN-DEGENERATE QUANTUM DOT CIRCUIT

A. Mapping onto the one-orbital non spin-degenerate case

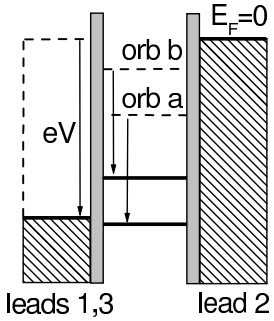

FIG. 19: Electrochemical potentials for a quantum dot connected to three paramagnetic leads and subject to no magnetic field, with two different orbitals levels a and b accessible for current transport.

We now consider the quantum dot circuit of Fig. 1 with $V > 0$, connected to paramagnetic leads ($P_1 = P_2 = P_3 = 0$) and with no magnetic field ($B = 0$). We assume that two different orbitals levels a and b of the dot are accessible for current transport, but we still consider that the dot cannot be doubly occupied. We define $\gamma_{j,orb}$ as the net tunneling rate between lead j and the orbital $orb \in \{a, b\}$. This problem is spin-degenerate and can thus be treated without the spin degree of freedom, which is replaced by the orbital degree of freedom. The rate for an electron to tunnel between lead j and the orbital level orb in direction ϵ is $\Gamma^{\epsilon}_{j,orb} = \gamma_{j,orb}/(1 + \exp[\epsilon(E_{orb} - eV_j)/k_BT])$, where E_{orb} is the intrinsic energy of the orbital level orb. This problem can be treated in the sequential tunneling limit with a Master equation analog to (3). There is in fact a direct mapping between this problem and that described in Section II. We will assume that $E_a < E_b$, so that the orbitals a and b will play the roles of the Zeeman sublevels $\uparrow$ and $\downarrow$ of Section II, where $B > 0$. One has to

replace the parameters of the previous problem by

$$\begin{aligned} E_{\uparrow(\downarrow)} &\longrightarrow E_{a(b)} \ , \\ \gamma_j &\longrightarrow \frac{\gamma_{j,a}+\gamma_{j,b}}{2} \ , \\ P_j &\longrightarrow \widetilde{P}_j = \frac{\gamma_{j,a}-\gamma_{j,b}}{\gamma_{j,a}+\gamma_{j,b}} \ , \\ \gamma_{\uparrow\downarrow(\downarrow\uparrow)} &\longrightarrow \gamma_{ab(ba)} \ . \end{aligned} \tag{40}$$

This mapping shows that one can obtain a super-Poissonian F_2 or a positive F_{13} in this two-orbital system. This result demonstrates that interactions can lead to zero-frequency positive cross-correlations in a normal quantum dot circuit even *without lifting spin-degeneracy*. Note that in practice, $\gamma_{j,a} = \gamma_{j,b}$ is not obvious because of the different spatial extensions of the orbitals (see for instance [39, 53]). This problem is thus equivalent to a one-orbital problem with $B \neq 0$ *and* with finite effective polarizations $\widetilde{P}_1, \widetilde{P}_2, \widetilde{P}_3$ which can be close to ± 1. Positive cross-correlations can be expected either at the resonance associated to level b (for $E_b < 0$) or in the plateau following this resonance, depending on the parameters (see for instance Fig. 18).

B. Comments

In the one-orbital ferromagnetic case, we have shown that the simple relation (25) between F_2 and F_{13} is valid in the high-voltage limit only when $P_1 = P_3$. Therefore, according to the mapping indicated in Section V.A., in the two-orbital case, relation (25) is valid in the high-voltage limit only if $\widetilde{P}_1 = \widetilde{P}_3$ i.e. $\gamma_{1,a}/\gamma_{3,a} = \gamma_{1,b}/\gamma_{3,b}$. Hence, the conditions of validity of property (25) found in Section II.D for the one-orbital system (i.e. same polarization for the two output leads and high-voltage limit) cannot be generalized to the two-orbital case.

In the spin-degenerate case treated here, positive cross-correlations stem from the partial blockade of an electronic channel by another one, thus we suggest to call this effect: *dynamical channel-blockade*. This effect should be observable in semiconductor quantum dots. The advantage of taking $B = 0$ is that the problem of spurious lead polarization evoked in Section IV is suppressed. When $eV \gg |E_b + E_C|$ and $\gamma_{sf} = 0$, the two channels conduct current independently, thus dynamical channel-blockade is suppressed and the positive cross-correlations disappear (see (40)+[48]). When $\Delta E \ll k_B T$, cross-correlations are always negative in a spin-degenerate three-terminal quantum dot placed in the sequential tunneling limit [28]. Therefore, our hypothesis $\Delta E \gg k_B T$ is also necessary to obtain positive cross-correlations in this device. In fact, when $\Delta E \ll k_B T$, the electron leaving the dot at a given time is not necessarily the one which entered the dot just before, in spite of $eV \ll E_C$: channel effects are suppressed.

Note that a super-Poissonian Fano factor can also be obtained in a spin-degenerate circuit based on two bi-terminal quantum dots (or localized impurity states) placed in parallel and coupled electrostatically to each other [64–66]. If one of the dots is charged, the other cannot transport current because of the Coulomb repulsion. The dot which changes its occupancy with a lower rate modulates the current through the other one, which leads to a dynamical channel-blockade analogous to what we found. The possibility to get positive cross-correlations in these systems was not investigated, but Section V of the present article suggests it.

VI. CONCLUSION

We have considered noise in a three-terminal quantum dot operated as a beam splitter. In this system, a super-Poissonian input Fano factor is not equivalent to zero-frequency positive output cross-correlations. We have studied three different ways to get these two effects, due to the mechanism of dynamical channel-blockade. The first two strategies consist in involving only one orbital of the dot in the electronic transport and lifting spin-degeneracy, either by using ferromagnetic leads or by applying a magnetic field to the dot. We have furthermore shown that lifting spin degeneracy is not necessary anymore when two orbitals of the dot are involved in the current transport. These results show that one can get zero-frequency positive cross-correlations due to interactions inside a beam splitter circuit even if this is a spin-degenerate normal fermionic circuit with a perfect voltage-bias.

We thank H. A. Engel, K. Ensslin, M. Governale, H. Grabert, R. Hanson, T. Kontos, R. Leturcq, B. Reulet, I. Safi, P. Samuelsson and B. Trauzettel for interesting discussions. We are particularly indebted to M. Büttiker for raising the question which led us to consider the case treated in Section V. This work was financially supported by the RTN Spintronics, by the Swiss NSF and the NCCR Nanoscience.

[1] Ya. M. Blanter and M. Büttiker, Phys. Rep. **336**, 1 (2000).
[2] *Quantum Noise in Mesoscopic Physics*, edited by Yu. V. Nazarov (Kluwer, Dordrecht, 2003).
[3] V. A. Khlus, Sov. Phys. JETP **66**, 1243 (1987).
[4] G. B. Lesovik, JETP Lett. **49**, 592 (1989).
[5] M. Büttiker, Phys. Rev. Lett. **65**, 2901 (1990).
[6] M. Büttiker, Phys. Rev. B **46**, 12485 (1992).
[7] M. Henny, S. Oberholzer, C. Strunk, T. Heinzel, K. Ensslin, M. Holland, and C. Schönenberger, Science **284**, 296 (1999).
[8] W. D. Oliver, J. Kim, R. C. Liu, and Y. Yamamoto, Science **284**, 299 (1999).

[9] S. Oberholzer, M. Henny, C. Strunk, C. Schönenberger, T. Heinzel, K. Ensslin, and M. Holland, Physica E **6**, 314 (2000).

[10] See the article of M. Büttiker, in Ref. [2].

[11] T. Martin, Phys. Lett. A **220**, 137 (1996).

[12] M. P. Anantram and S. Datta, Phys. Rev. B **53**, 16390 (1996).

[13] J. Torres and T. Martin, Eur. Phys. J. B **12**, 319 (1999).

[14] T. Gramespacher and M. Büttiker, Phys. Rev. B **61**, 8125 (2000).

[15] J. Torres, T. Martin, and G. B. Lesovik, Phys. Rev. B **63**, 134517 (2001).

[16] M. Shechter, Y. Imry, and Y. Levinson, Phys. Rev. B **64**, 224513 (2001).

[17] J. Börlin, W. Belzig, and C. Bruder, Phys. Rev. Lett. **88**, 197001 (2002).

[18] P. Samuelsson and M. Büttiker, Phys. Rev. Lett. **89**, 046601 (2002).

[19] P. Samuelsson and M. Büttiker, Phys. Rev. B **66**, 201306 (2002).

[20] F. Taddei and R. Fazio, Phys. Rev. B **65**, 134522 (2002).

[21] D. Sánchez, R. López, P. Samuelsson, and M. Büttiker, Phys. Rev. B **68**, 214501 (2003).

[22] G. Bignon, M. Houzet, F. Pistolesi, and F. W. J. Hekking, cond-mat/0310349.

[23] C. Texier and M. Büttiker, Phys. Rev. B **62**, 7454 (2000).

[24] M. Gattobigio, G. Iannaccone, and M. Macucci Phys. Rev. B **65**, 115337 (2002).

[25] A. M. Martin and M. Büttiker, Phys. Rev. Lett. **84**, 3386 (2000).

[26] I. Safi, P. Devillard, and T. Martin, Phys. Rev. Lett. **86**, 4628 (2001).

[27] A. N. Korotkov, Phys. Rev. B **49**, 10381 (1994); S. Hershfield, J. H. Davies, P. Hyldgaard, C. J. Stanton, and J. W. Wilkins, *ibid.* **47**, 1967 (1993); U. Hanke, Yu. M. Galperin, K. A. Chao, and N. Zou, *ibid.* **48**, 17209 (1993).

[28] D. A. Bagrets and Yu. V. Nazarov, Phys. Rev. B **67**, 085316 (2003).

[29] H. Birk, M. J. M. de Jong, and C. Schönenberger, Phys. Rev. Lett. **75**, 1610 (1995); H. Birk, K. Oostveen, and C. Schönenberger, Rev. Sci. Instrum. **67**, 2977 (1996).

[30] B. R. Bulka, J. Martinek, G. Michalek, and J. Barnas, Phys. Rev. B **60**, 12246 (1999); B. R. Bulka, Phys. Rev. B **62**, 1186 (2000).

[31] E. V. Sukhorukov, G. Burkard, and D. Loss, Phys. Rev. B **63**, 125315 (2001).

[32] D. V. Averin, in *Macroscopic Quantum Coherence and Quantum Computing*, edited by D. V. Averin, B. Ruggiero, and P. Silvestrini (Kluwer, Dordrecht, 2001); cond-mat/0010052.

[33] F. Yamaguchi, and K. Kawamura, Physica (Amsterdam) **227B**, 116 (1996); G.-H. Ding and T.-K. Ng, Phys. Rev. B **56**, R15521 (1997); Y. Meir and A. Golub, Phys. Rev. Lett. **88**, 116802 (2002).

[34] A. Cottet, W. Belzig, and C. Bruder, Phys. Rev. Lett **92**, 206801 (2004).

[35] A. Cottet and W. Belzig, Europhys. Lett. **66**, 405 (2004).

[36] W. Belzig and M. Zareyan, Phys. Rev. B **69**, 140407(R) (2004).

[37] M. Julliere, Phys. Lett. A **54**, 225 (1975).

[38] H. A. Engel and D. Loss, cond-mat/0312107.

[39] R. Leturcq, D. Graf, T. Ihn, K. Ensslin, D. Driscoll, and A. C. Gossard (unpublished).

[40] M.M. Deshmukh, and D. C. Ralph, Phys. Rev. Lett. **89**, 266803 (2002); M. M. Deshmukh, E. Bonet, A. N. Pasupathy, and D. C. Ralph, Phys. Rev. B **65**, 073301 (2002).

[41] Note that $n_b = I_{2\uparrow}/I_{2\downarrow}$ includes bunches with no up spins, i.e. two down spins passing consecutively. Thus, n_b can be smaller than 1.

[42] Note that despite this, we have chosen to show in Sections II.A and II.B curves for the case $\gamma_3/\gamma_1 = 10$ because it allows to get, just by reversing the polarization of one output lead, both the cases where $S_{13}(\omega = 0)$ is positive or negative while F_2 is super-Poissonian.

[43] R. J. Soulen Jr., J. M. Byers, M. S. Osofsky, B. Nadgorny, T. Ambrose, S. F. Cheng, P. R. Broussard, C. T. Tanaka, J. Nowak, J. S. Moodera, A. Barry, and J. M. D. Coey, Science **282**, 85 (1998).

[44] D. C. Glattli, P. Jacques, A. Kumar, P. Pari, and L. Saminadayar, J. Appl. Phys. **81**, 7350 (1997).

[45] M. R. Buitelaar, A. Bachtold, T. Nussbaumer, M. Iqbal, and C. Schönenberger, Phys. Rev. Lett. **88**, 156801 (2002)

[46] K. Tsukagoshi, B. W. Alphenaar, and H. Ago, Nature. **401**, 572 (1999).

[47] O. Sauret and D. Feinberg, Phys. Rev. Lett. **92**, 106601 (2004).

[48] In the one-orbital case, positive cross-correlations can be obtained only if the tunneling rates for one spin direction depend on the occupation of the other spin level. When charging effects are not relevant, i.e. $V \gg |E_\uparrow + E_C|\, C/(C_1 + C_3)$ for $E_0 > 0$ or $V \gg |E_\downarrow + E_C|\, C/C_2$ for $E_0 < 0$, the tunneling rates become independent of the occupation of the dot and one can check that for $\gamma_{sf} = 0$, $S_{13}(\omega = 0)$ is always negative for any polarization of the leads 1, 2, 3.

[49] A. K. Hüttel, H. Qin, A. W. Holleitner, R. H. Blick, K. Neumaier, D. Weinmann, K. Eberl, and J. P. Kotthaus, Europhys. Lett. **62,** 712 (2003).

[50] G. Schmidt, D. Ferrand, L. W. Molenkamp, A. T. Filip, and B. J. van Wees, Phys. Rev. B **62**, R4790 (2000); A. Khaetskii, J. C. Egues, D. Loss, C. Gould, G. Schmidt, and L. W. Molenkamp, cond-mat/0312705.

[51] A. Thielmann, M. H. Hettler, J. König, and G. Schön, Phys. Rev. B **68**, 115105 (2003).

[52] P. Recher, E.V. Sukhorukov, and D. Loss, Phys. Rev. Lett. **85**, 1962 (2000).

[53] R. Hanson, L. M. K. Vandersypen, L. H. Willems van Beveren, J. M. Elzerman, I. T. Vink, and L. P. Kouwenhoven, cond-mat/0311414.

[54] D. C. Ralph, C. T. Black, and M. Tinkham, Phys. Rev. Lett. **74**, 3241 (1995); *ibid.* **78**, 4087 (1997).

[55] D. H. Cobden, M. Bockrath, P. L. McEuen, A. G. Rinzler, and R. E. Smalley, Phys. Rev. Lett. **81**, 681 (1998); D. H. Cobden and J. Nygard, *ibid.* **89**, 046803 (2002).

[56] R. Hanson, B. Witkamp, L. M. K. Vandersypen, L. H. Willems van Beveren, J. M. Elzerman, and L. P. Kouwenhoven, Phys. Rev. Lett. **91**, 196802 (2003).

[57] A. V. Khaetskii and Yu. V. Nazarov, Phys. Rev. B **61**, 12639 (2000); *ibid.* **64**, 125316 (2001); S. I. Erlingsson and Yu. V. Nazarov *ibid.* **66**, 155327 (2002).

[58] M. Ciorga, M. Pioro-Ladriere, P. Zawadski, P. Hawrylak, and A. S. Sachrajda, Appl. Phys. Lett. **80**, 2177 (2002).

[59] M. C. Rogge, C. Fuhner, U. F. Keyser, and R. J. Haug, cond-mat/0310469.

[60] W. Lu, Z. Ji, L. Pfeiffer, K. W. West, and A. J. Rimberg, Nature **423**, 422 (2003).

[61] M. Field, C. G. Smith, M. Pepper, D. A. Ritchie, J. E. F.

Frost, G. A. C. Jones, and D. G. Hasko, Phys. Rev. Lett. **70**, 1311 (1993).
[62] J. M. Elzerman, R. Hanson, J. S. Greidanus, L. H. Willems van Beveren, S. De Franceschi, L. M. K. Vandersypen, S. Tarucha, and L. P. Kouwenhoven, Phys. Rev. B **67**, 161308(R) (2003).
[63] R. Schleser, E. Ruh, T. Ihn, K. Ensslin, D. C. Driscoll, and A. C. Gossard (unpublished).
[64] S. S. Safonov, A. K. Savchenko, D. A. Bagrets, O. N. Jouravlev, Y. V. Nazarov, E. H. Linfield, and D. A. Ritchie, Phys. Rev. Lett. **91**, 136801 (2003).
[65] G. Kießlich, A. Wacker, and E. Schöll, Phys. Rev. B **68**, 125320 (2003).
[66] A. Nauen, F. Hohls, J. Könemann, and R. J. Haug, cond-mat/0402358.